



Advances in TiS₂ for energy storage, electronic devices, and catalysis: A review



Yunhong Jiang^{a,*}, Heping Xie^a, Lu Han^{b,***}, Yuan Zhang^{a,d}, Yanhuai Ding^c, Suling Shen^a,
Bin Chen^{a,**}, Meng Ni^d

^a Guangdong Provincial Key Laboratory of Deep Earth Sciences and Geothermal Energy Exploitation and Utilization, Institute of Deep Earth Sciences and Green Energy, Shenzhen University, Shenzhen, 518060, China

^b School of High Temperature Materials and Magnesite Resources Engineering, University of Science and Technology Liaoning, 185 QianshanZhong Road, Anshan, 114044, China

^c Institute of Rheological Mechanics, Xiangtan University, Hunan, 411105, China

^d Department of Building and Real Estate, Research Institute for Sustainable Urban Development, The Hong Kong Polytechnic University, Hong Kong, China

ARTICLE INFO

Keywords:

TiS₂
Morphology control
Energy storage and conversion
Electronic devices
Catalysis

ABSTRACT

As the lightest family member of the transition metal disulfides (TMDs), TiS₂ has attracted more and more attention due to its large specific surface area, adjustable band gap, good visible light absorption, and good charge transport properties. In this review, the recent state-of-the-art advances in the syntheses and applications of TiS₂ in energy storage, electronic devices, and catalysis have been summarized. Firstly, according to the physical presentation of the TiS₂ synthesis reaction, it can be divided into a solid phase synthesis, a liquid phase synthesis and a gas phase synthesis. Secondly, we summarize the applications of TiS₂ in energy storage, electronic devices and catalytic: (1) The applications of TiS₂ nanostructure in energy storage direction from the aspects of Li-ion battery (LIB), Li-S battery (LSB), Na-ion battery (NIB), K-ion battery (KIB), Mg-ion battery (MIB), solar cells and hydrogen storage; (2) The applications of TiS₂ nanostructures in various electronic devices from thermoelectric devices, high power lasers and flexible devices; (3) Applications based on energy catalysis and environmental catalysis. Based on the various synthetic technologies and wide applications of TiS₂, we firmly believe that the challenges of TiS₂ will be solved and become a hot star material in the future. Finally, we discuss the future scope and the current challenges arising from this fascinating material.

1. Introduction

Since Geim successfully isolated single-layer graphite by micro-mechanical exfoliation method, two-dimensional (2D) materials have become a hot topic in the field of materials science [1]. However, because graphene is a zero bandgap material, the use of graphene in field effect transistors and logical devices has been limited [2]. Recently, transition metal disulfides (TMDs) with a chemical formula of MS₂ (where M = Mo, Ti, W, Nb, etc.) have attracted great interest because of their direct bandgap, tunable interlayer space, and nonlinear optical properties [3]. TMDs can serve as metallic, half-metallic, semiconducting, and superconducting materials, which depends on their d-electron number of M and crystal structures. In the crystal structure of TMDs, two layers of S

atoms are intercalated by a layer of M atoms. M – S is strongly covalent-bonded, while the interaction between MS₂-MS₂ layers is weak van Der Waals forces. Thus, single- and few-layer MS₂ can be isolated from bulk materials by chemical and mechanical exfoliation method.

After the discovery of graphene, molybdenum disulfide (MoS₂) has become the most studied material in the TMDs family due to its structural similarity to graphene. Due to its high carrier transport, low cost, and tunable bandgap, MoS₂ has been explored in various applications such as energy storage and conversion, photocatalysis, and environmental remediation. Since the beginning of 1977, titanium disulfide (TiS₂) has been widely concerned by researchers since its application in lithium-ion battery (LIB) anodes [4–8]. TiS₂ exhibits a semimetallic to semiconducting behavior, depending on the its form from bulk to monolayer

* Corresponding author.

** Corresponding author.

*** Corresponding author.

E-mail addresses: joyhonhong@outlook.com (Y. Jiang), hanlu@ustl.edu.cn (L. Han), chenbin@szu.edu.cn (B. Chen).

structure [9]. Theoretical calculations reveal the conduction band minimum and valence band maximum of monolayer TiS_2 appear partially overlapping, and its band structure can be modulated by strain engineering [9,10]. However, a semiconducting behavior can be observed in monolayer TiS_2 under nonstrain conditions. The tiny nonstoichiometric feature induces the discrepancy of electronic structure between the theoretical calculation data and experimental data. It has been demonstrated that the physical properties of TiS_2 rely on the number of layers, suggesting that the electrical structure can be tuned by adjusting the layer number. The Ti atomic layer in TiS_2 is sandwiched between two tightly arranged S atomic layers, which then form the S–Ti–S structural morphology. (Fig. 1a) [11–13]. Single layer TiS_2 extracted from natural bulk form has been found either in octahedral (1 T) or hexagonal (2H) phase [14]. The 1 T phase is more energetically stable than the 2H phase using density functional theory (DFT) calculations. The mechanical properties of TMDs are crucial for the durability and performance of the

device. The Young's modulus of TiS_2 (1 T) nanotube with a diameter of 8–9 nm is about 228 GPa, and Young's modulus of monolayer TiS_2 reaches 85.20 N/m [15]. The mechanical properties of TiS_2 calculated by DFT method is greatly dependent on the size and structure of the calculation models. Monolayer TiS_2 is well recognized as a good electrode material for rechargeable metal ion battery due to the high metal ion adsorption energies and low diffusion barriers. The theoretical capacity of TiS_2 reaches 957.2 mAhg^{-1} and 1914 mAhg^{-1} for alkali metal (Na, Li and K) ions and alkaline earth metal ions (Mg and Ca), respectively [14]. 2D TiS_2 has broad spectral absorption properties from visible to infrared bands, which can be employed to develop nonlinear photonic devices [16].

The band structure of TiS_2 calculated by DFT is shown in Fig. 1b and c. The highest valence band of TiS_2 is between A and L with an indirect overlap of about 0.11 eV [17]. The lowest energy band from -14.1 to -11.2 eV is mainly composed of the 3p orbital of S. The upper Fermi level

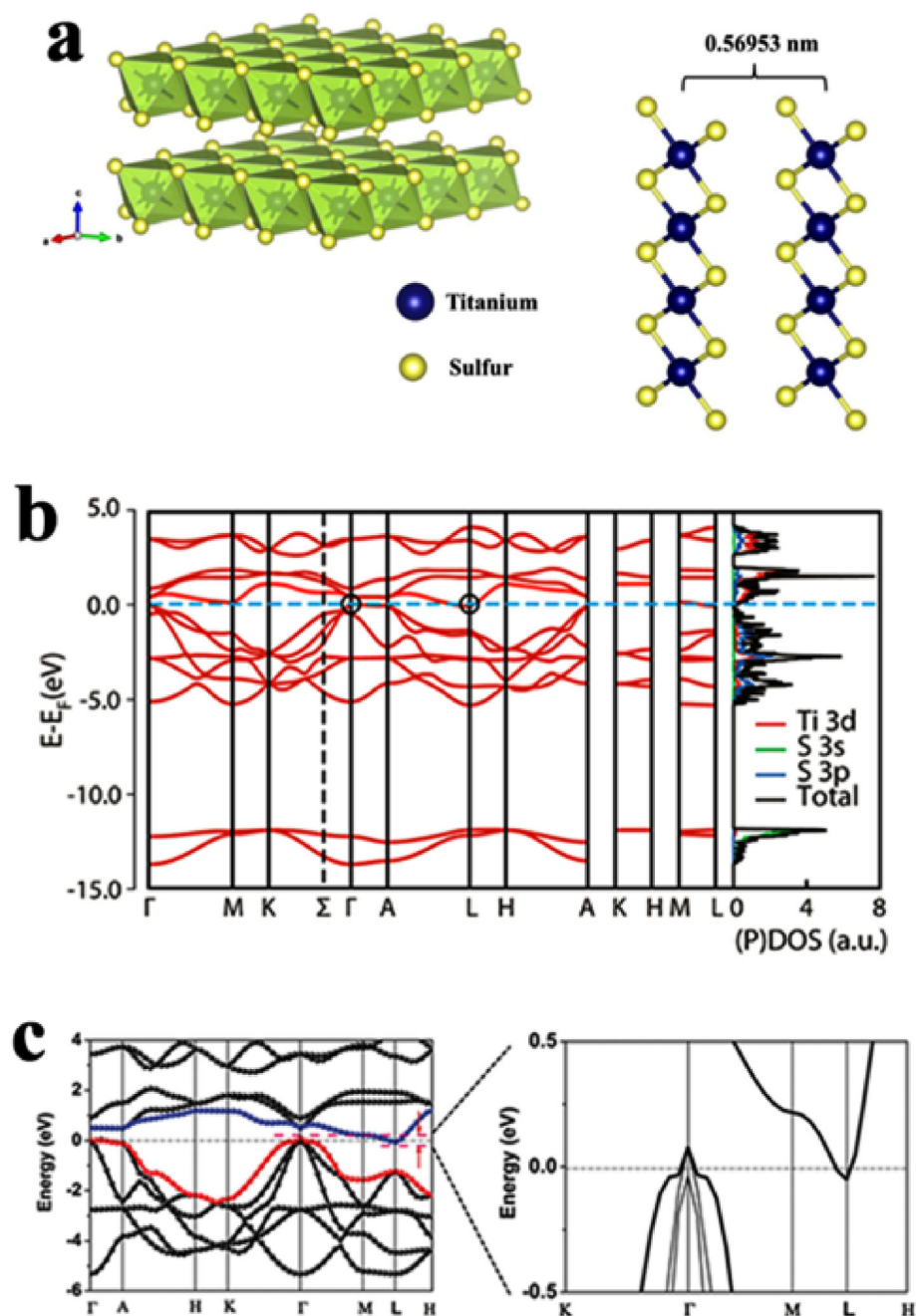


Fig. 1. a) Simulated crystal structure of TiS_2 (ICSD 5295) showing layered morphology of the compound (left); a stick-ball model of TiS_2 crystal structure depicting the inter-layer spacing in a typical TiS_2 crystal. Band structure of TiS_2 . b) Electronic band structure along high-symmetry directions (left) and DOS (right) of TiS_2 at optimized lattice parameters (strain-free system). c) Calculated energy band structure of 2D TiS_2 by density functional theory, indicating the semimetal characteristics [12,17,19].

is from 0 eV to 5 eV, and the 0.7, 1.9 and 3.0 peaks are composed of 3d orbital of Ti. The density of states of the Fermi level is occupied by the 3p orbital of the hybridized S and the 3d orbital of Ti. This hybridization results in the calculated density of states can not reach the vicinity of the 0 Fermi level, indicating TiS_2 is a semimetal material. Hall measurements show that TiS_2 has n-type carriers at high electron concentration. The resistivity of TiS_2 decreases with decreasing temperature due to the increase of carrier Hall mobility. From experimental measurements and theoretically, it is concluded that overwhelmingly, TiS_2 is a typical semimetal material [17–21].

Up to now, following the upsurge of interest in graphene, wide applications of TiS_2 in electrochemical energy storage, solar energy utilization, catalytic and electronic devices have been explored. To our knowledge, there is no systematic review on the synthesis and application of TiS_2 nanostructures. As shown in Fig. 2, this paper summarizes the synthesis methods and application status of TiS_2 , and points out some potential research directions of TiS_2 .

2. Synthesis of TiS_2

In recent years, a lot of research has been done on the synthetic methods of two-dimensional materials, which provides ideas for the effective synthesis of TiS_2 , and tries to find an effective and controllable method to prepare TiS_2 with specific properties by using different synthetic techniques. Generally, the preparation of layered TiS_2 can be divided into solid phase synthesis, liquid phase synthesis, and gas phase synthesis according to its physical state, which are applied in different fields according to its inherent characteristics. The three synthetic methods are briefly described below.

2.1. Solid phase synthesis

The most common method for preparing TiS_2 is high-temperature solid-phase reaction, which has the advantages of simple production process, large-scale production, and controllable cost. Various nanomaterials have been produced by high-temperature solid-phase synthesis, such as TiO_2 [22–24], ZnO [23,25,26], MoS_2 [23,27], TiS_2 [17,23], and so on. In particular, it has become the main method for synthesizing layered TiS_2 , which significantly promotes the study of layered TiS_2 . As

shown in Fig. 3a and b, in a typical one-step solid phase reaction, Ti and S powder are uniformly mixed and placed in a quartz tube, then vacuum sealed and heat-treated at a high temperature [6,28–32]. In order to obtain TiS_{2-x} , a certain amount of TiS_2 is placed on one side of the Y-shaped quartz tube, and the other side is passed through a certain amount of Ti powder to absorb sulfur vapor at a high temperature [33, 34]. Other vapors such as iodine can also be used as the transmission medium [35]. The product prepared by this method presents platelet-like morphology as shown in Fig. 3c [30].

Fig. 3d and e demonstrate the synthesis of typical TiS_3 nanoribbon arrays. The Ti source was first sputtered onto the carbon-coated Al(C–Al) foil with the assistance of a magnetron sputtering system to form a thin film, which was then successively loaded into the same quartz tube along with the S powder. The quartz tube needs to be vacuumed and heated in an oven for a few hours before being flame sealed, then it is removed and quickly quenched. Next, the TiS_3 nanoribbons need to be converted into TiS_{2-x} nanoribbons. The conversion process requires placing the prepared substrate with TiS_3 coating and an appropriate amount of Ti powder into a new quartz tube, where glass wool plugs can be used as isolation plate to prevent direct contact of the Ti powder with the TiS_3 substrate during processing and sealing. The new quartz tube containing the TiS_3 substrate and Ti powder was evacuated and flame sealed under vacuum. The sealed quartz tube was then treated at high temperature for several hours and cooled to room temperature to obtain TiS_{2-x} nanoribbons [28,34]. The specific morphological features of TiS_{2-x} nanoribbons can be observed in Fig. 3f–i. The TiS_2 powder particles synthesized by high-temperature solid-phase reaction have no agglomeration, uniform particle size, high crystallinity, and generally exhibit 2H phase. Therefore, it can be suitable for applications in energy storage, energy conversion, and electron transport.

2.2. Liquid phase synthesis

Compared with the high-temperature solid phase synthesis strategy, the liquid phase synthesis strategy has great advantages in controlling the morphology and size of nanomaterials, and it has higher production efficiency at lower energy consumption [36,37]. At present, a variety of nano materials have been prepared by liquid phase synthesis strategy, such as various metals [38,39], metal oxides [38,40,41], and metal sulfides [38,42–45]. In particular, various layered nanomaterials have been successfully prepared by a liquid-phase synthesis strategy, which has promoted the research on TiS_2 .

Fig. 4a demonstrates the liquid-phase synthesis of TiS_2 nanocrystals. In an argon atmosphere, CS_2 (or S powder) and oleylamine were added to a three-necked flask. The mixture in the three-necked flask was pre-treated for a period of time to remove air and other impurities. After purging with argon, when the reaction temperature reached 250–300 °C, TiCl_4 was injected into the reaction mixture. After a period of time, the reaction was stopped and cooled to normal temperature naturally. Then, excess butanol was added to the reacted mixture and centrifuged to obtain the desired TiS_2 crystal powder. The obtained powder was thoroughly washed in a mixed solution of ethanol and ethane, and collected. As shown in Fig. 4b, different sized of TiS_2 nanocrystals can be obtained by varying the concentration of the reactants, and the size distribution is between several tens of nanometers and two hundred nanometers [16, 32,46–48].

TiS_2 nanotubes can be prepared by the following procedure: Place $\text{Na}_2\text{S}\cdot 9\text{H}_2\text{O}$ on P_2O_5 and vacuum anneal at 200 °C for sufficient time to remove crystal water. Meanwhile, tetrahydrofuran (THF) was refluxed in the presence of $\text{LiAlH}_4\cdot 8\text{THF}$ for a period of time and then distilled under an argon atmosphere to obtain a pure THF solution. Then the TiCl_4 and pure THF solution were mixed in an anhydrous and oxygen-free environment to form a new solution. Then Na_2S without water of crystallisation was added to the new solution at 40 °C with constant stirring. After the reaction was completed, it was cooled to room temperature, and thoroughly washed with a mixed solution of THF and methanol to obtain

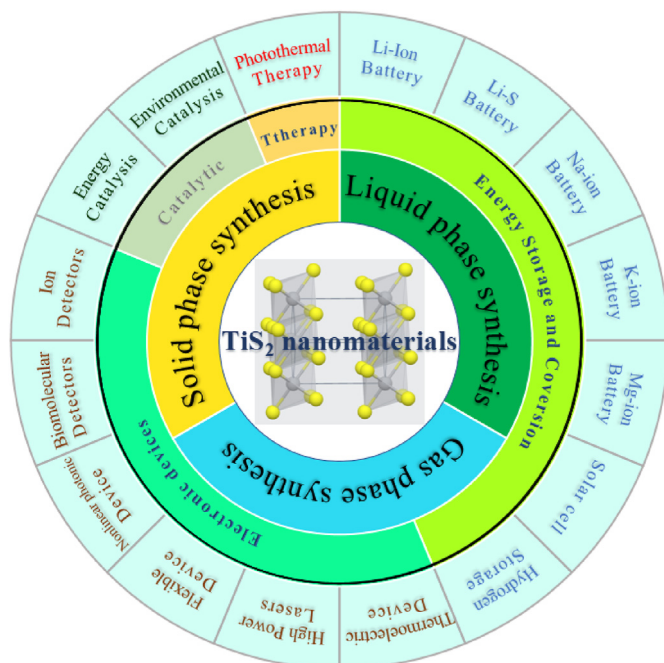


Fig. 2. Synthetic methods and application diagrams of TiS_2 nanomaterials.

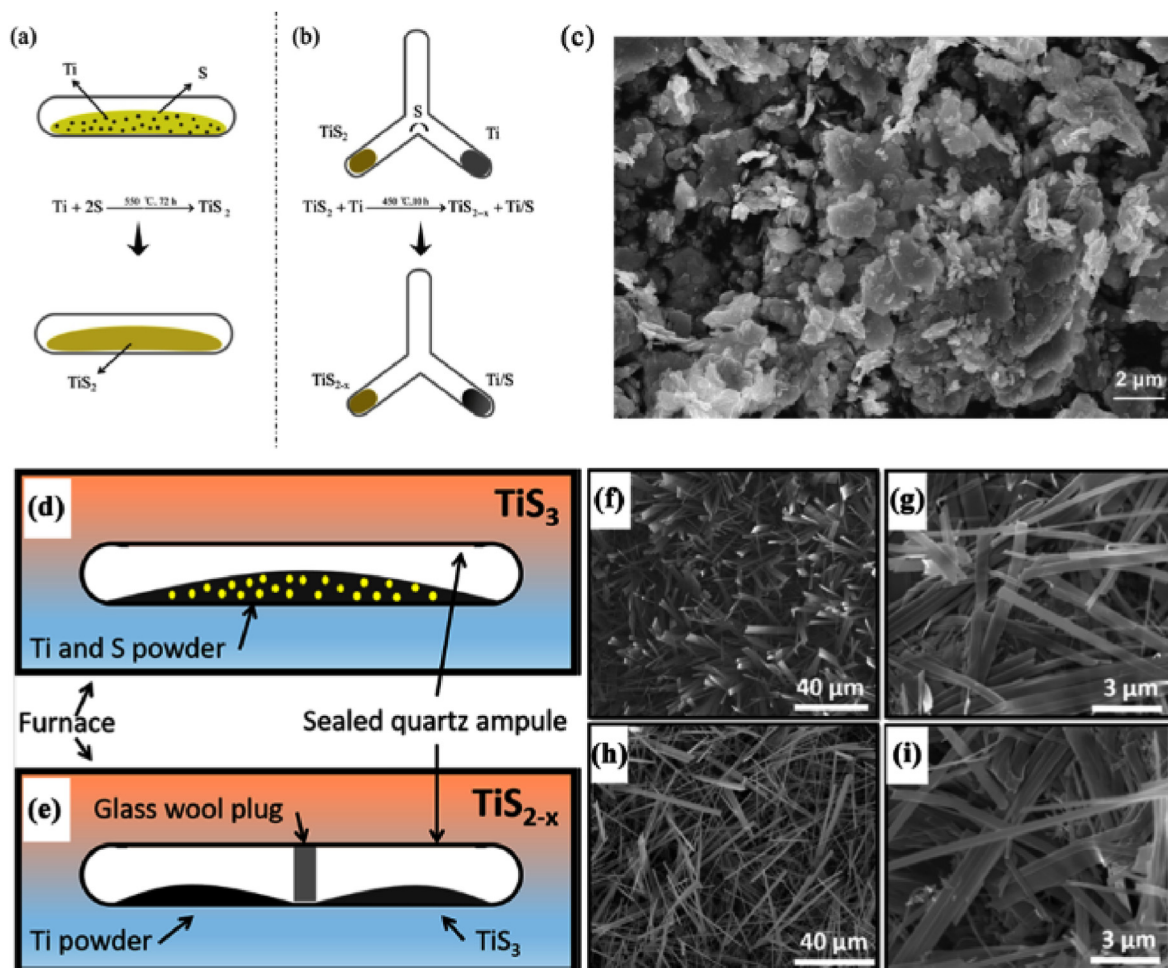


Fig. 3. Schematic illustration of the synthesis pathways of (a) TiS_2 , (b) TiS_{2-x} . (c) SEM image of TiS_2 showing its platelet morphology. Schematic depiction of the arrangement of the sealed quartz ampule for the synthesis of TiS_3 (d) and TiS_{2-x} (e) nanobelts. SEM images of TiS_3 (f, g) and TiS_{2-x} (h, i) nanobelts [30,33,34].

a dark brown solid powder. The powder was rinsed in a H_2 atmosphere at 200 °C for a period of time to remove the solvent, and at the same time pure TiS_2 nanotubes were obtained. The multi-walled structure of TiS_2 nanotubes can be observed in Fig. 4c [49].

In the liquid phase synthesis strategy, in addition to preparing TiS_2 in solvent, TiS_2 with a certain nano-morphology can also be synthesized by a simple molten salt method. As shown in Fig. 4d, TiS_2 nanosheets with large size and ultrathin were synthesized by molten salt interfacial reaction [50]. In a typical reaction, quantities of anhydrous Na_2S , NaCl , and KCl are mixed well and transferred into a quartz reactor with a graphite steel pot. The reactor was thoroughly washed with argon to remove interfering gases such as oxygen, and then TiCl_4 gas and argon were introduced at the same time and annealed. The annealing temperature was controlled between 700 °C and 850 °C. After reacting for a period of time and cooling to room temperature, the target TiS_2 nanosheets can be obtained. The SEM image of TiS_2 nanosheets is shown in Fig. 4e. As shown in Fig. 4f, TiS_2 nanosheets can also be prepared by mechanical milling followed with a liquid-phase exfoliation process. A suitable amount of a mixture of Li_3N and TiS_2 was mechanically ground at room temperature. TiS_2 nanosheets were prepared by liquid phase stripping of the prepared mixture of Li_3N and TiS_2 . In all procedures, exposure to ambient air was avoided by sealing the sample under argon [51].

The TiS_2 prepared by the liquid phase synthesis strategy has controllable nano-morphological characteristics, which is a feasible method for the preparation of ultrathin TiS_2 . Therefore, this method can be used to regulate the morphology of TiS_2 , increase its specific surface area and electron transport performance, and enhance its application in

extreme electron transport and extreme energy conversion.

2.3. Gas phase synthesis

Although the gas phase synthesis is rarely used in the preparation of TiS_2 , this method has the advantages of high production precision, small product size, etc. As shown in Fig. 5a, the gas-phase synthesis of TiS_2 used a vertically designed apparatus as the reactor instead of the commonly used horizontal apparatus. This apparatus allows TiCl_4 and H_2S gases to flow in opposite directions in the reactor and contact the reaction, while the temperature is controlled between 650 and 850 °C. A filter several tens of degrees lower than its temperature was placed under the reactor to collect the TiS_2 powder. Among them, TiCl_4 vapor can be generated by the device shown in Fig. 5b, and the temperature of the precursor in the apparatus is controlled at about 120 °C. It can be found in Fig. 5c and d that TiS_2 prepared with this device exhibits a closed cage-like structure. As shown in Fig. 5e, appropriate reduction of the synthesis reaction temperature can reduce the size of TiS_2 [52].

TiS_2 nanomaterials, such as TiS_2 whiskers, can also be obtained using a conventional horizontal device. First, a thin layer of Ni metal catalyst is firmly supported on one side of the Si wafer. Then, the Si wafer was placed above the quartz boat filled with an appropriate amount of Ti powder, and the Ni metal layer and the Ti powder had a certain distance for the steam to flow. Next, another quartz boat containing S powder was placed upstream of the gas flow of the pipeline, heated to above 600 °C under the protection of argon gas flow, reacted for a period of time to cool and collect the Si wafer substrate. As shown in Fig. 5f–i, the TiS_2

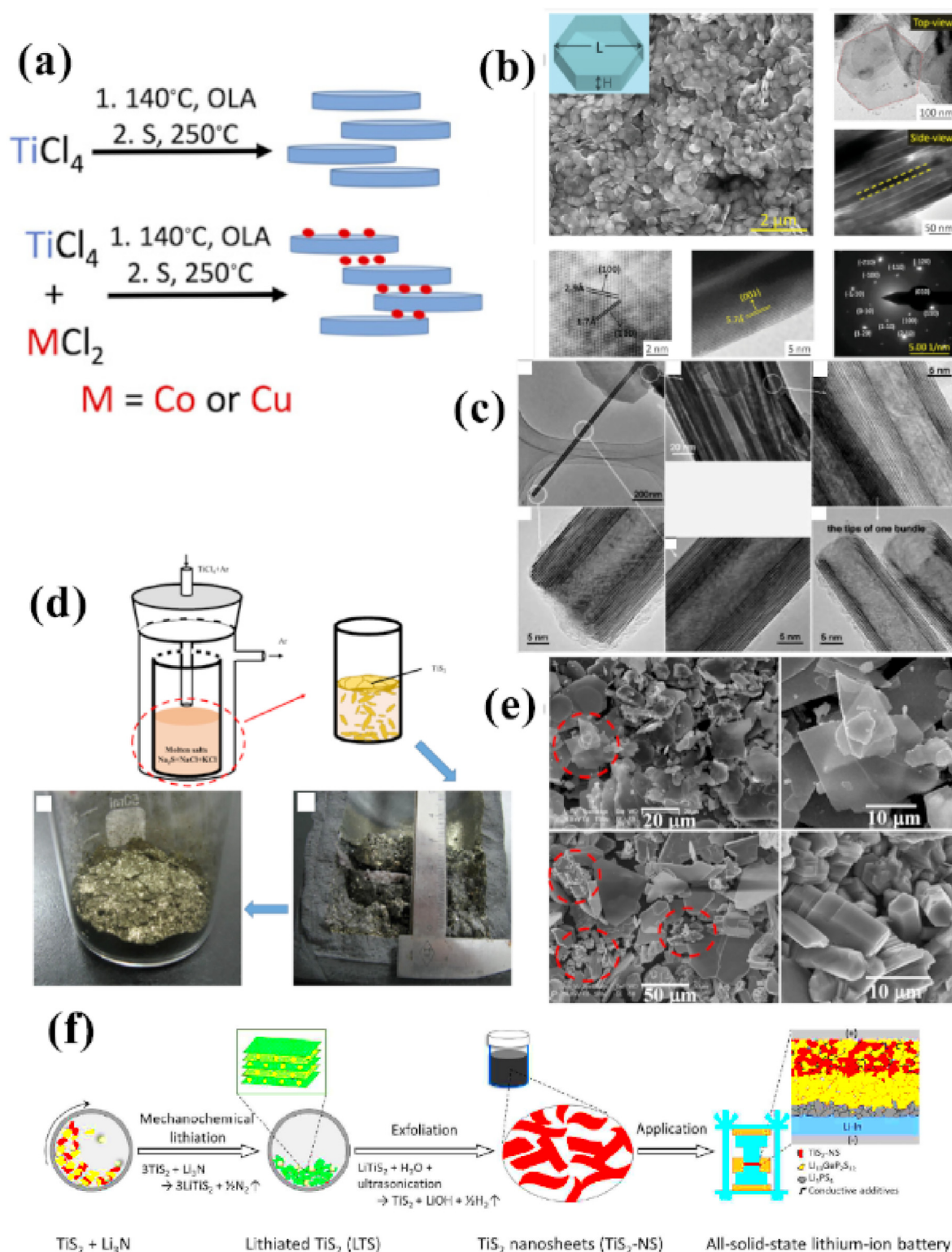


Fig. 4. (a) The synthetic scheme for TiS₂ materials. (b) SEM images of TiS₂ NSs, inset shows the 3D morphology of a single TiS₂ NS, the size and thickness of which are defined as L and H, respectively. Top-view and side-view low-resolution TEM images of TiS₂ NSs. Corresponding top-view and side-view high-resolution TEM images. Detailed selected area electron diffraction (SAED) of a single TiS₂ NS. (c) Representative low-magnification and high-resolution TEM images of multiwalled TiS₂ nanotubes. (d) Schematic showing the synthesis of TiS₂ flakes by the gas/liquid reaction between TiCl₄ and S²⁻ in molten NaCl-KCl melts. Cross section of the cooled graphite crucible after completion of the reaction. Typical optical photo of the collected TiS₂ flakes prepared at 750 °C. (e) SEM images of as-synthesized TiS₂ at 750 °C for 5 h; the enlarged image of the dash circle part in; at 850 °C for 6 h and represent high-resolution image of the aggregated small particles as shown in the dash circle parts. (f) Schematic diagram illustrating preparation of TiS₂ nanosheets (TiS₂-NS) and their application in bulk-type all-solid-state lithium-ion batteries (ASLBs) using sulphide SEs [17,49–51].

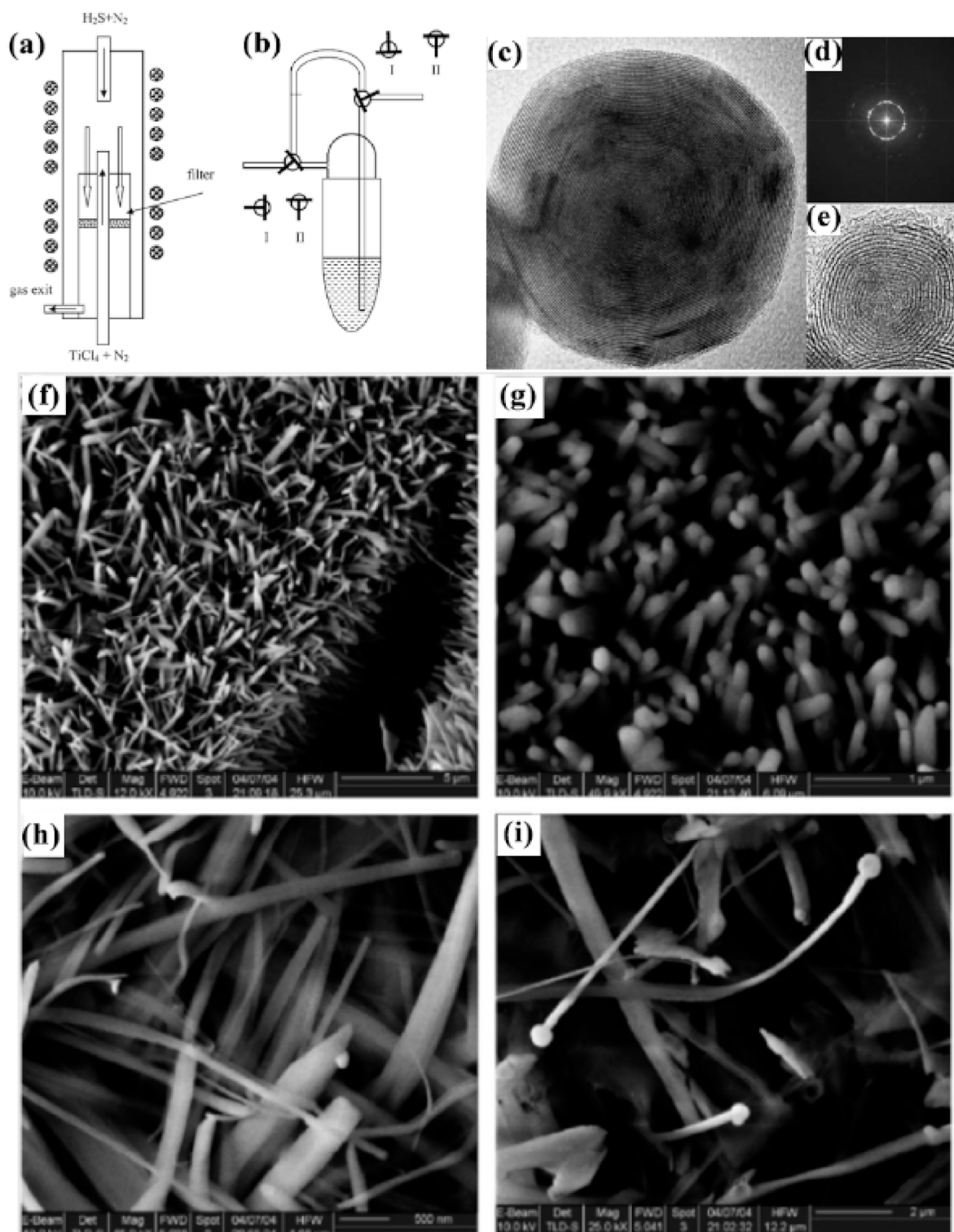


Fig. 5. (a) Schematics of the reactor, used for the synthesis of IF-TiS₂. (b) The gas-washing bottle with a bypass, used for the advanced preparation of the precursor: 'I' is the valve position used for flushing the system with pure nitrogen gas; 'II' is the position of the valves during the reaction. This bypass prevents the flow of the highly reactive TiCl₄ precursor during the heating up and cooling down steps of the synthesis. (c) TEM image of a typical IF-TiS₂ nanoparticle. The interlayer distance is 5.8 Å and the diameter of the nanoparticle is larger than 70 nm. (d) The fast fourier transform (FFT) of the nanoparticle. (e) TEM image of the small (20 nm) TiS₂ nanoparticle, received in the low-temperature synthesis (650 °C). Note the almost complete empty hollow core. The interlayer distance is 5.8 Å. (f) and (g) Low magnification SEM image of TiS₂ whiskers; (h) high magnification SEM image of TiS₂ whiskers; and (i) whisker terminate with a nanoparticle implying the VLS mechanism for TiS₂ whisker [52,53].

whiskers were grown uniformly and vertically on the Si wafer [53]. Tuning the connection configuration of the gas-phase synthesis device can also control the morphology of TiS_2 nanomaterials. The TiS_2 sample synthesized by the gas phase reaction have a small particle size and generally exhibits a 1 T phase. 1 T- TiS_2 has interesting physical properties such as pressure-induced superconducting phase transition and single-layer charge density wave phase transition, and is considered as a model material for Fermi liquids. Studying the fundamental electronic structure and properties of 1 T- TiS_2 materials is of great significance for understanding quantum physics phenomena, single-layer charge density wave phase transition mechanisms, and exploring potential applications in advanced electronic and optoelectronic devices.

We briefly summarize several synthetic methods including solid phase reaction, liquid phase reaction and gas phase reaction for the synthesis of TiS_2 nanomaterials. From these synthetic methods, we can see that solid phase synthesis is the easiest and most common used method. This method has the advantages of simple production process, high production efficiency and low cost. We believe that the large scale preparation of TiS_2 nanostructure by using this method can be achieved recently. However, solid phase reaction is relatively difficult in morphology control, as most of the synthesized products are irregular block or particle structures with small specific surface area, which is not conducive to the stability of energy storage materials and the charge transfer of electronic devices and catalytic reactions. However, liquid and gas phase reactions can easily control the morphology of TiS_2 under certain conditions, such as TiS_2 nanodisks and TiS_2 nanowhiskers, and even monolayer TiS_2 materials. These materials with small dimensions and large specific surface area often have good photoelectric conversion performance and relatively stable ion storage capacity. Therefore, we hope to explore the synthesis methods of TiS_2 nanostructures with smaller dimensions and larger specific surface area in the future, in order to improve the performance of TiS_2 nanomaterials in various applications.

3. Application of TiS_2

In this section, we will focus on the main applications of TiS_2 and make a brief analysis of its potential applications based on its excellent performance and novel features.

3.1. Energy storage and conversion

With the continuous pursuit of the quality of daily life and the depletion of fossil energy, the energy issue has become one of the most important issues in today's society [17,54–57]. In the past decade, the prices of traditional fuels have been rising, and energy storage and conversion have become a major concern in the world. Therefore, how to use high-tech electrochemical energy storage technology to solve this problem has more potential than ever before, such as rechargeable battery technology, fuel cell technology and solar cell technology [27,33,58]. Here, we will summarize some of the research results of TiS_2 from the perspective of energy storage and conversion.

3.1.1. Li-ion battery

LIBs are clearly the most successful compared to other energy storage devices since Sony commercialized them [25,51,59,60]. Over the past few decades, LIBs have found numerous applications in devices such as mobile phones, laptops, electric vehicles, and smart grids. However, the safety and durability issues of commercial LIBs have not been well solved [4,27,61]. How to improve its durability and efficiency on the basis of ensuring safety has become the main problem currently faced by LIBs. Therefore, it is necessary to select suitable electrode materials and technologies to ensure that they are commercially viable and sufficiently safe [28,59,62].

Because of their ideal theoretical capacity, transition metal sulfides have become popular electrode materials for LIBs [28,63]. As a typical

transition metal sulfide, TiS_2 has the advantages of high energy density (239 mA h g^{-1}), low discharge voltage (2.1 V), fast ion separation speed, and small volume expansion, and is a potential electrode material for LIBs [64,65]. The application of TiS_2 -based electrode materials in LIBs has been extensively studied [12,28,34]. Zhang et al. [66] conducted a systematic study on the chemical reaction mechanism of TiS_2 as an electrode by operating in situ X-ray absorption spectroscopy combined with DFT calculations. The comparison of specific capacity before and after 100 cycles clarifies that the charge-discharge of TiS_2 is a highly reversible intercalation reaction. During the charging and discharging process, transfer electrons exist on both the Ti 3 d orbital and the S 3p orbital, which proves the participation of Ti and S in the redox reaction process of the electrode. However, the intercalation reaction of TiS_2 is only partially reversible during the first charge-discharge cycle. However, as the number of electrode cycles increases, the reversible reaction becomes more complete. However, if the cycle is continued, Ti–O related compounds will be generated inside the electrode, thereby reducing the reversibility of the intercalation reaction and the capacity fading. In addition, after further cycling, the carbonate formed in the solid-electrolyte interfacial layer gradually loses its activity, which eventually also leads to a rapid capacity decay.

Casey G et al. [34] converted TiS_3 nanoribbons into TiS_{2-x} nanoribbons by a nondestructive desulfurization procedure and carefully studied their structural and optoelectronic properties. The study confirmed that the transformed TiS_{2-x} nanoribbons have typical metallic properties. Furthermore, the non-stoichiometric TiS_{2-x} nanoribbons exhibit excellent electrochemical performance on the basis of their special physical properties. Not only has high specific capacity, but also has sustainable capacity retention. Thus, TiS_2 optimized nanostructures are promising materials for high-power, stable and long-life LIBs. TiS_2 can also be used as the anode for LIBs with “water-in-salt” electrolytes. Sun et al. [67] took advantage of the excellent properties in the “water-in-salt” electrolyte not only to improve the electrochemical reversibility of TiS_2 , but also to effectively suppress side reactions during charge and discharge. Their pair-assembled full cells using LiMn_2O_4 and TiS_2 exhibited high energy density and discharge voltage, and also exhibited considerable rate capability.

In addition, TiS_2 materials also have considerable prospects in the application of solid-state LIBs [56,62,63]. Unemoto et al. [59] successfully achieved 300 charge-discharge cycles using an all-solid-state battery composed of a LiBH_4 electrolyte and a TiS_2/Li paired electrode. The battery has a high specific capacity and reaches 85% of the theoretical capacity of TiS_2 . Even after 300 cycles, the discharge specific capacity can reach 88% of the second cycle, showing good charge-discharge stability. The better stability can be attributed to the stable interface between the TiS_2 and LiBH_4 electrolytes, which was confirmed to have highly inert $\text{Li}_2\text{B}_{12}\text{H}_{12}$.

3.1.2. Li–S battery

Because of the high theoretical energy density of Li–S batteries, they have received much attention in the field of electric vehicles. S is one of the ideal materials for large-scale application of energy storage devices because of its abundant reserves and low cost [33,68]. However, in general, lithium-sulfur batteries have lower effective energy utilization and faster capacity decay. The main reason for this is that S and Li react to form an intermediate called polysulfide rather than an ideal end product (Li_2S) [69–71].

Therefore, to avoid the interference of intermediate products, sulfur and the soluble polysulfides it forms must be restricted to the cathode of Li–S batteries [68,72]. Currently, the study of S cathode structure can be divided into two categories: (1) based on mesoporous or microporous carbon nanostructures, which can retain a large amount of S; (2) Additives containing polysulfides [33,68,73]. These two types of structures either physically or chemically limit the outward diffusion of polysulfides, resulting in improved energy efficiency and cycle stability. Of course, these structures also increase the proportion of inactive materials,

which reduces the overall energy density. Therefore, researchers hope to find a multifunctional structure or additive that can provide additional capacity to increase the energy density of cathode materials [33]. One of the typical examples of multifunctional cathode additives is TiS_2 . Next, we will discuss the latest progress in the study of TiS_2 as a multifunctional cathode additive.

Manthiram et al. [68] developed a simple and practical cathode material consisting of a mixture of TiS_2 and polysulfides to improve the inherent electrochemical instability and low efficiency of Li-S batteries, as well as to avoid undue manufacturing parameters such as low S content. TiS_2 functions as a conductive polymer adsorbent in the composite electrode. To demonstrate the excellent polymer stability and high load capacity of the mixtures, they encapsulated the electrochemically stable TiS_2 -polysulfide mixture in a carbon electrode. Fig. 6a depicts the manufacturing process for a mixed TiS_2 -polysulfide cathode. Fig. 6b and c shows the SEM images of the fresh and recycled mixed cathodes after 200 cycles, respectively. Fig. 6d–i shows the electrochemical properties of hybrid cathodes. Through adsorption simulation experiments and electrochemical measurements, Zhao et al. [33] showed that TiS_{2-x} promoter has better S adsorption capacity than TiS_2 , which is helpful to inhibit the shuttle effect, accelerate the reaction kinetics of Li and S, and improve the charging and discharging performance and service life of Li-S batteries. Huang et al. [74] synthesized a sandwich-like ultra-thin TiS_2 nanosheet by a new method. Its special porous structure is very good for adsorption of polysulfides, thus improving the utilization rate of S.

3.1.3. Na-ion battery

The Na-ion batteries (NIBs) have attracted great attention from related industries because of their large storage capacity, low cost, low toxicity and environmental friendliness [28,75]. Especially recently CATL released a comprehensive push on the use of sodium ion batteries in electric vehicles. However, the major challenge facing NIBs at present is to find high capacity and high power electrode materials [76]. Because both the mass and radius of Na ions are larger than that of Li ions, the influence of voltage lag is greater, resulting in a relatively poor power of NIBs [55,77]. Most of the high performance electrode materials that can

be used normally in LIBs batteries are no longer suitable for NIBs, such as graphite [47,75,77]. However, TMDs found in recent years still have great potential in NIBs battery system.

Because TMD materials are connected by weak van der Waals forces and have large spacing between layers along the vertical direction of the [0001] two-dimensional interface, sodium ions can be easily stored and released in the middle of this atomic layer, and their volume will not change much during storage and release. NIBs assembled from low-cost TMD materials such as MoS_2 , SnS_2 , WS_2 and TiS_2 have been shown to have recyclable potential and good charge-discharge performance [31, 47,55].

Han et al. [55] successfully observed the Na insertion into TiS_2 nanotables using in situ TEM. Local volume expansion and a small amount of structural breakdown occurred at the edge of TiS_2 lattice because the rate of original sodium embedded phase boundary was greater than the rate of migration at the transition phase boundary, resulting in a deterioration of performance during the cycle. About a quarter of the cells in each atomic plane are occupied by sodium, resulting in the superstructure of 2×2 . When sodium is embedded, a repulsive force is formed, which effectively reduces the formation of this superstructure, resulting in the destruction of its structure. Tang et al. [78] designed a special carbon-coated TiS_2 nano-tablet for NIBs. The NIBs assembled with this material has ideal charging and discharging performance, rate performance and cyclic stability up to 5000 times. They believe this is due to the synergistic effect between the intrinsic properties of TiS_2 and the sodium ion intercalation mechanism. Hu et al. [75] synthesized ultra-thin TiS_2 nanosheets using a simple shear mixer and showed good performance in NIBs applications. Like Tang et al. they explained the reason why the electrodes had excellent electrochemical properties in mechanism.

3.1.4. K-ion battery

Compared with other alkali metal ion batteries, K-ion Battery (KIBs) have some unique advantages. First, potassium can be uniformly deposited on the electrode surface. Secondly, KIBs have higher open circuit voltage than NIBs and other batteries. Then, potassium is

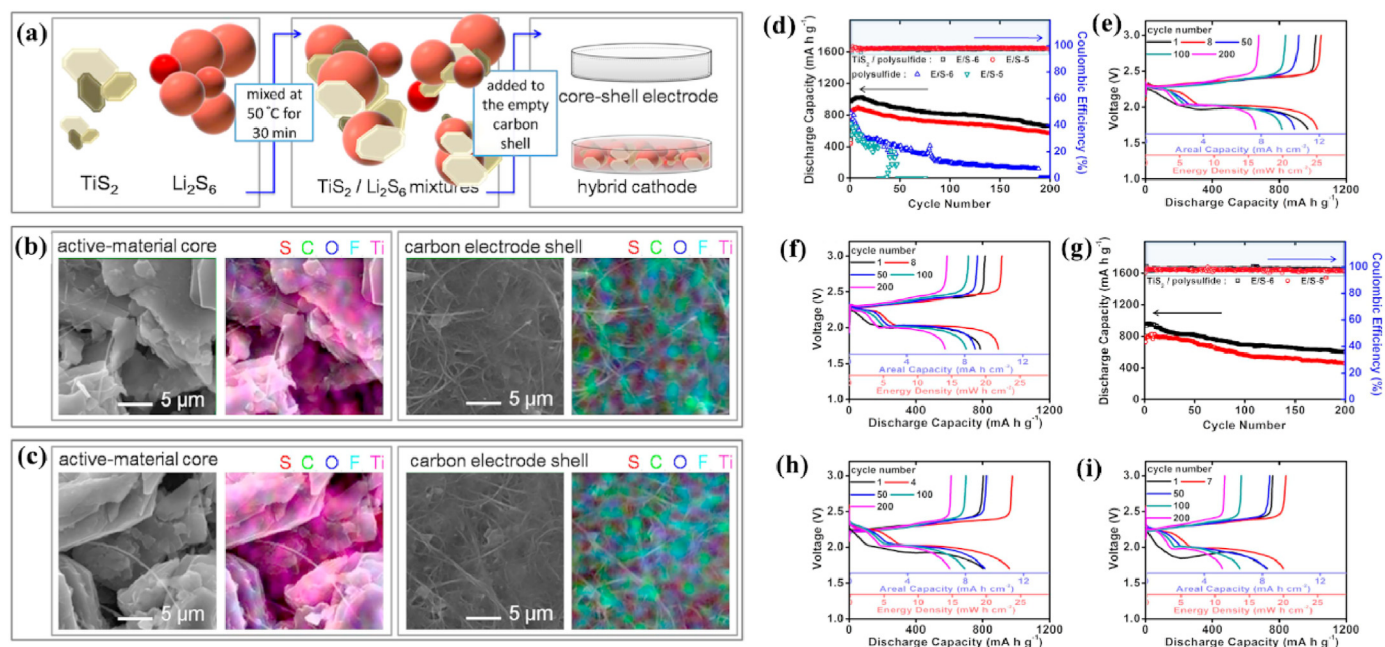


Fig. 6. (a) Schematic fabrication process of the hybrid TiS_2 -polysulfide cathode. Microstructural analysis with SEM and EDX of the (b) freshly made cathode and (c) cycled cathode after 200 cycles. Cell performance of the hybrid cathodes and a control cathode with a sulfur loading of 12 mg cm^{-2} , sulfur content of 65 wt %, and sulfur mass of 12mg/cathode at low electrolyte/sulfur ratios of 6 and $5 \mu\text{L mg}^{-1}$. (d) Cyclability analysis at a C/10 rate and the corresponding discharge/charge curves of the hybrid cathodes with electrolyte/sulfur ratios of (e) 6 and (f) $5 \mu\text{L mg}^{-1}$. (g) Cyclability analysis at a C/5 rate and the corresponding discharge/charge curves of the hybrid cathodes with electrolyte/sulfur ratios of (h) 6 and (i) $5 \mu\text{L mg}^{-1}$ [68].

abundant on the earth. In addition, KIBs can use aluminum foil to replace copper foil to reduce cost. Wang et al. [8] applied layered TiS_2 cathode material to KIBs. The battery assembled with it and ether based electrolyte has excellent charge discharge performance and rate performance. They found that ether based electrolytes have higher charge transfer rates and ionic conductivity than carbonate based electrolytes. Liu et al. [79] made some defects on the surface of TiS_2 through specific methods, and believed that such functional defects could alleviate the volume expansion, thus improving the stability of its assembled battery, and its dynamic performance was also improved. At the same time, they also proved this view through calculation.

3.1.5. Mg-ion battery

Mg-ion battery (MIBs) have higher volume energy density, better safety and lower cost than LIBs. There is no dendrite growth during the charge and discharge process, and magnesium metal can also be directly used as a negative electrode to assemble batteries. Because layered TiS_2 can provide a stable charge discharge capacity of 115 mA h g^{-1} in MIBs, Sun et al. [30] consider it an ideal MIBs cathode material. They observed the staged insertion and uneven distribution of magnesium in the experiment, and thought that this phenomenon could make TiS_2 store more magnesium. Yoo et al. [80] also reported that the specific discharge capacity of TiS_2 nanotubes in the mixed magnesium lithium battery is 220 mA h g^{-1} at 0.1 C. Tao et al. [81] believed that the increase of active sites in TiS_2 materials could improve the charge discharge performance of MIBs batteries.

3.1.6. Solar cell

With the intensification of the world energy crisis and the enhancement of human awareness of environmental protection, solar power generation is considered as an important energy source in the next few hundred years due to its safety, pollution-free, simple maintenance, long life and abundant energy resources [82–84]. Since the 1980s, the photovoltaic industry formed by it has developed rapidly and become one of the fastest growing emerging industries in the world. As the core of photovoltaic industry, solar cells have received great attention and

achieved rapid development due to their high energy conversion efficiency and low manufacturing cost. The TiS_2 discussed in this paper has good application prospects in dye sensitized solar cells (DSSC) and perovskite solar cells (PSC) [85]. For examples, Huckaba et al. [46] synthesized a new low-cost hole transport material based on TiS_2 nanoparticles by a simple two-step thermal injection method. When applied to PSC, more than 13.5% of PCE can be obtained. Fig. 7a–c shows the structural layer of a perovskite solar cell device by low-cost TiS_2 as hole-transport Material. Fig. 7d–f shows the performance characteristics of perovskite solar cells with TiS_2 . Yin et al. [86] prepared TiS_2 nano-sheets by a simple solution stripping method and applied them as an effective electron transport layer to PSC, showing 17.37% of PCE. Huang et al. [87] used 2D TiS_2 prepared by stripping aqueous solution at room temperature as an electron transport layer in a planar *n*-i-p PSC. After inserting a 2D TiS_2 electron transport layer by UV-ozone treatment, the PCE of a planar PSC was optimized to 18.79%. In addition, Lickleder et al. [88] prepared highly catalytically active and conductive TiS_2 from TiO_2 nanotube arrays, and tested electrochemical activity as a counter electrode in DSSC. A PEC of 6.1% was obtained, which is very close to the reference value obtained for Pt (6.2%).

Due to its large specific surface area, unique interstitial void space and abundant electrochemical active sites, TiS_2 shows great potential in energy storage devices. In particular, the small size and thinness of TiS_2 allow them to adapt quickly and reliably to the intercalation cycle, making them particularly attractive for the manufacture of high performance batteries and capacitors. In Table 1, we summarize the electrochemical performance of TiS_2 and its composites. Electrochemical results confirm that layered TiS_2 materials may be suitable candidates for energy storage applications. On the other hand, TiS_2 nanomaterials play an important role in the hole or electron transport layer in PSCs and DSSCs.

3.2. Electronic devices

Ultra-thin 2D nanomaterials such as graphene and TMDs have received much attentions due to their microscopic compressibility and macroscopic scalability, which facilitate their applications in

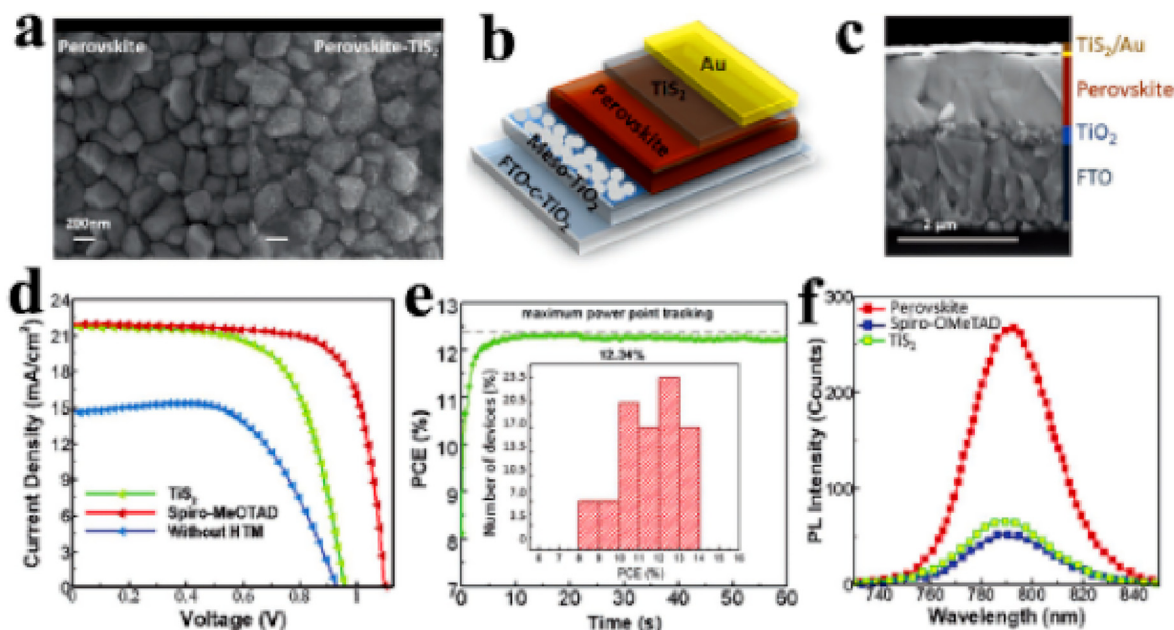


Fig. 7. a). Top-view SEM images for the perovskite film before and after deposition of TiS_2 nanoparticles. b,c) Device schematic (b) and cross-sectional SEM image (c) of a typical perovskite device. The different layers are identified on the right panel. d) J-V curve of the champion cells employing TiS_2 and spiro-OMeTAD as HTMs and no-HTM for comparison. e) Maximum power point tracking (MPPT) of one of the best performing devices based on TiS_2 HTM for 60s, which results in a stabilized power output of 12.34%. Inset: Histogram of PSC efficiencies obtained for more than 50 devices containing TiS_2 nanoparticles. f) Steady-state photoluminescence (PL) spectra of the perovskite material based on TiS_2 and spiro-OMeTAD as HTMs and no-HTM [46].

Table 1
Summary of electrochemical performance of TiS_2 and its composites in energy storage.

Material	Preparation Method	Application	Capacitance	Cycling stability	Ref.
TiS_2 powder	Commercial TiS_2	All-Solid-State Lithium Batteries	205 mA h g^{-1}	87.8% after 300 cycles	[59]
TiS_2 powder	Commercial TiS_2	All-Solid-State Lithium Batteries	278 mA h g^{-1}	78% after 600 cycles	[56]
TiS_2 powder	Commercial TiS_2	All-Solid-State Lithium Batteries	208 mA h g^{-1}	72% after 50 cycles	[63]
TiS_2 powder	Commercial TiS_2	All-Solid-State Lithium Batteries	220 mA h g^{-1}	89% after 40 cycles	[62]
TiS_2 powder	Commercial TiS_2	Aqueous Lithium Secondary Battery	140 mA h g^{-1}	45% after 40 cycles	[60]
TiS_2 powder	Commercial TiS_2	Aqueous Lithium Secondary Battery	270 mA h g^{-1}		[138]
TiS_2 powder	Commercial TiS_2	Aqueous Lithium Secondary Battery	130 mA h g^{-1}	80% after 20 cycles	[7]
TiS_2 powder	Commercial TiS_2	Calcium Ion Battery		Fundamental Studies	[139]
TiS_2 powder	Commercial TiS_2	$\text{LiMn}_2\text{O}_4/\text{TiS}_2$ full cell	58 mA h g^{-1}	74% after 50 cycles	[67]
TiS_2 nanobelts	Sputter sintering	Lithium and Sodium Ion Batteries	Li:225 mA h g^{-1} Na:217 mA h g^{-1}	99.5% after 100 cycles	[28]
TiS_2 powder	Commercial TiS_2	Lithium Ion Batteries	240 mA h g^{-1}	79% after 300 cycles	[140]
TiS_2 powder	Commercial TiS_2	Lithium Ion Battery	208 mA h g^{-1}	88% after 100 cycles	[34]
TiS_2 Nanobelts	Solid phase sintering	Lithium Ion Battery	225 mA h g^{-1}	90% after 100 cycles	[30]
TiS_2 Nanosheets	Commercial TiS_2	Lithium Ion Battery	291 mA h g^{-1}	98.7% after 50 cycles	[51]
TiS_2 single crystals	Solid phase sintering	Lithium Ion capacitors	212 mA h g^{-1} 131 F g^{-1}	99% after 120 cycles 95% after 500 cycles	[12]
TiS_2 powder	Commercial TiS_2	Lithium-Sulfur Batteries	825 mA h g^{-1}	83% after 200 cycles	[68]
Sulfur-Deficient TiS_{2-x}	Solid phase sintering	Lithium-Sulfur Batteries	1170 mA h g^{-1}	78.9% after 100 cycles	[33]
TiS_2 Nanosheets	Commercial TiS_2	Lithium-Sulfur Batteries	690 mA h g^{-1}	77% after 250 cycles	[69]
TiS_2 powder	Commercial TiS_2	Lithium-Sulfur Batteries	1000 mA h g^{-1}	96% after 40 cycles	[72]
TiS_2 powder	Commercial TiS_2	Magnesium and Calcium Ion Battery		Fundamental Studies	[141]
Layered TiS_2	Solid phase sintering	Magnesium Ion Battery	140 mA h g^{-1}	82% after 40 cycles	[25]
TiS_2 powder	Commercial TiS_2	Potassium Ion Battery	145 mA h g^{-1}	87% after 120 cycles	[54]
TiS_2 powder	Commercial TiS_2	Potassium ion battery	80 mA h g^{-1}	79% after 600 cycles	[8]
TiS_2 Nanosheets	Solid phase sintering	Sodium Ion Batteries	386 mA h g^{-1}	175% after 250 cycles	[75]
TiS_2 powder	Solid phase sintering	Sodium Ion Batteries	1040 mA h g^{-1}	336% after 9000 cycles	[31]
TiS_2 powder	Solid phase sintering	Sodium Ion Batteries	146 mA h g^{-1}	100% after 50 cycles	[6]
TiS_2 powder	Commercial TiS_2	Sodium Ion Batteries	210 mA h g^{-1}	71% after 40 cycles	[142]
TiS_2 nanoplates	Hot injection	Sodium Ion Batteries	188 mA h g^{-1}	76% after 300 cycles	[47]
TiS_2 powder	Commercial TiS_2	Sodium Ion Batteries		Fundamental Studies	[55]
TiS_2 single crystals	Solid phase sintering	Sodium Ion Batteries	148 mA h g^{-1}	85% after 50 cycles	[77]

nanoelectronic devices. TiS_2 is a highly conductive material with a graphene like structure and is therefore an ideal candidate for graphene and TMDs [89]. Layered TiS_2 has proven to be an excellent material for electronic devices, a variety of applications of TiS_2 , including thermoelectric devices, high power lasers, memory devices, ultra-pulse

generation and all-optical threshold devices, as well as biomolecular detectors and Ion detector, have been explored in recent years.

3.2.1. Thermoelectric device

Unlike the previous energy storage devices, thermoelectric devices do

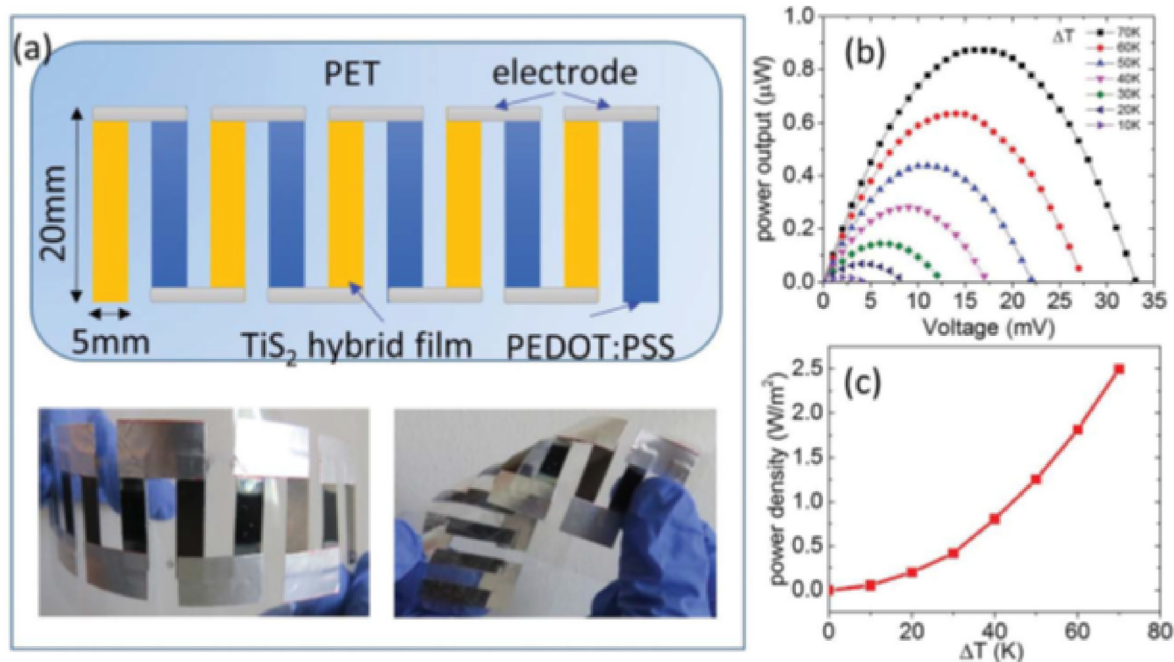


Fig. 8. (a) Our prototype thermoelectric devices composed of a p-type PEDOT:PSS film and n-type TiS_2 /organic superlattice film, both being deposited onto the flexible PET substrate. (b) The generated power output at different temperature gradients. (c) The calculated power density as a function of the temperature gradient [92,93].

not need to be charged frequently or replaced due to performance degradation, which makes them a power supply device that can be built on a larger scale. The thermoelectric materials with high power factor and performance play a key role in the thermoelectric device. Light, flexible, non-toxic and high-performance materials are desired for advanced c [90,91]. Researchers are paying much attention to TiS_2 because of its high thermoelectric performance, low material cost, controllability and high mechanical flexibility. Tian et al. [92] proposed a simple stripping and recombination method to prepare a flexible film hybridized by TiS_2 and organic compounds. This flexible film shows a special lattice structure consisting of alternating layers of TiS_2 and organic molecules stacked along the c-axis. Because the addition of organic molecules promotes charge transfer, the conductivity of this flexible film has been greatly improved. At the same time, the Seebeck coefficient can be further improved by properly annealing this film in vacuum environment. As shown in Fig. 8a–c, such material is deposited on a permeable PET substrate and the module is free to bend or twist. Wan et al. [93] The inorganic layer is injected outside the thermoelectric material, and then the organic cations are used to stabilize electrons, so as to provide n-type carriers for electron transport and energy transfer during operation. This hybrid superlattice is more mechanically elastic than TiS_2 single crystal. The bending modulus measured at 300 K is about 145 MPa, which is much lower than that of TiS_2 single crystal, even lower than some common plastic materials. When the device assembled with three materials is attached to the surface of glass tubes of different sizes, it shows that it has high sensitivity. In order to further understand the current application of TiS_2 and its composites in thermoelectric devices, we have simply summarized the research achievements in recent years in Table 2, and compared their power factor (PF) and thermoelectric performance (ZT).

3.2.2. High power lasers

The rapid development of high power lasers has promoted the industry's demand for efficient optical restraint materials to protect eyes and sensors. TMD materials with unique structure have attracted much attention in many applications including optical confinement due to their excellent physical and chemical properties. The optical limiting effect of some TMD materials is even smaller than that of fullerene (C60) and graphene. As shown in Fig. 9a and b, Varma et al. [94] studied the optical

limiting activity of TiS_2 and graphene slices using an improved method and compared them with C60. The optical restriction activity observed in TiS_2 nanotablets was greater than that observed in C60 and graphene. It is believed that the process of induced excitation state absorption and two-photon absorption in TiS_2 sheet promotes the enhancement of optical restriction activity. This idea has been confirmed by corresponding measurement techniques, providing evidence for the use of TiS_2 nano-materials as potential candidates for photoelectric applications. Li et al. [95] demonstrated a passively Q-switched Er:YAG laser at 1645 nm using a prepared TiS_2 saturated absorber (Fig. 9c–e), and it has a pulse energy of 37.4 μJ under certain conditions, so they believe that the TiS_2 saturable absorber is an important candidate for the preparation of optical modulators. Tian et al. [96] prepared multilayer TiS_2 by easy liquid phase stripping. This multilayer TiS_2 can be used as an alternative material for an effective light modulator because of its ultra-fast non-linear optical response caused by unbalanced electrons and helps the effective light modulator to obtain ultra-fast optical lasers near the optical communication band. Using this effective light modulator, they observed a stable femtosecond mode-locked spectrum.

3.2.3. Flexible devices

Flexible electronic devices have attracted much attention as one of the development directions of electronic devices in the future. As a result, concepts such as wearable devices [97,98], medical implantable devices [99], electronic skin [100] and smart electronic fabrics [101] have been proposed continuously, which form part of the blueprint of human life in the future. With the rapid development of flexible wearable electronic technology, electronic equipment has gradually evolved from a rigid system to a flexible system, and finally to a flexible wearable electronic product. In recent years, the field of flexible electronic devices has been expanded due to the rapid development of flexible high-temperature superconducting film and wearable resistance-switched memory [102, 103]. Lin et al. [29] succeeded in preparing a novel hydrogenated TiS_2 nanosheet with less than five atomic layers by an effective chemical stripping method. Hydrogenated TiS_2 achieves unprecedented high conductivity in assembled films up to $6.76 \times 10^4 \text{ S/m}$ at 298 K, which is even better than the traditional conductive ITO. The high pressure tolerance and transfer mode for transferrable assembled hydrogenated TiS_2 film are illustrated in Fig. 10a–d. Lyu et al. [104] obtained a

Table 2

Summary of TiS_2 and its composites in thermoelectric devices.

Material	Preparation Method	ZT	PF	Ref.
Al:[TiS_2 nanosheets]	Commercial TiS_2 SPS		216.7 $\mu\text{W/m K}^2$ at 298 K	[143]
TiS_2 superlattice	Commercial TiS_2 and liquid exfoliation	0.17 at 298 K	210 $\mu\text{W/m K}^2$ at 298 K	[92]
Te/ TiS_2 nanocables	Hydrothermal PVD	1.91 at 300 K	0.58 mW/m K^2 at 30 K	[144]
TiS_2 single crystal	liquid exfoliation self-assembly process	0.12 at 393 K	1.15 mW/m K^2 at 300 K	[145]
PbS nanoparticle embedded TiS_2	Solid phase sintering SPS	0.5 at 573–673 K	1.23 mW/m K^2 at 573–673 K	[146]
Copper intercalated TiS_2	Solid phase sintering SPS	0.45 at 800 K	1.7 mW/m K^2 at 325 K	[147]
Cu_xTiS_2 ceramics	Solid phase sintering SPS	0.5 at 800 K	1.9 mW/m K^2 at 800 K	[148]
$(\text{SnS})_{1-2}(\text{Cu}_{0.02}\text{Ti}_{0.98}\text{S}_2)_2$	Solid phase sintering SPS	0.42 at 720 K	0.68 mW/m K^2 at 720 K	[149]
$(\text{SnS})_{1-2}(\text{Co}_{0.02}\text{Ti}_{0.98}\text{S}_2)_2$				
$(\text{BiS})_{1-2}(\text{TiS}_2)_2$	Solid phase sintering SPS	0.3 at 750 K	0.69 mW/m K^2 at 750 K	[150]
$x\text{MoS}_2\text{-TiS}_2$	Solid phase sintering SPS	0.29 at 573 K	1 mW/m K^2 at 573 K	[151]
$\text{TiS}_2\text{-xPbSnS}_3$	Solid phase sintering SPS	0.44 at 650 K	1.45 mW/m K^2 at 500 K	[152]
$\text{Co}_{0.04}\text{TiS}_2\text{ Ta}_{0.1}\text{Ti}_{0.9}\text{S}_2$	Solid phase sintering SPS	no change at 300 K		[153]
$\text{Co}_x\text{Ti}_{1-x}\text{S}_2$	Solid phase sintering SPS	0.0293 at 310 K	3.93 $\mu\text{W/cm K}^2$ at 310 K	[154]
$\text{Ti}_{1-x}\text{Nb}_x\text{S}_2$	Solid phase sintering SPS	0.24 at 700 K	0.69 mW/m K^2 at 700 K	[155]
$\text{TiS}_2\text{:Sn}_x$	Solid phase sintering Secondary sintering	0.46 at 623 K	1.53 mW/m K^2 at 623 K	[156]
$(\text{SnS})_{1-2}(\text{TiS}_2)_2$	Solid phase sintering centrifugal heating	0.23 at 623 K		[157]
$\text{Ti}_{1-x}\text{Nb}_x\text{S}_2$	Solid phase sintering Mechanically alloyed	0.3 at 700 K	1.6 mW/m K^2 at 300 K	[158]
$(\text{SnS})_{1-2}(\text{TiS}_2)_2$	Solid phase sintering SPS	0.37 at 700 K	0.97 mW/m K^2 at 523 K	[159]
$\text{TiS}_2(\text{HA})_{0.096}(\text{EG})_{0.31}$	Solid phase sintering electrochemical intercalation	0.17 at 298 K		[160]
$\text{TiS}_2[(\text{HA})_{0.08}(\text{H}_2\text{O})_{0.22}(\text{DMSO})_{0.03}]$	Solid phase sintering electrochemical intercalation	0.28 at 373 K	0.45 mW/m K^2 at 298 K	[93]
$\text{TiS}_2(\text{HA})_x$	Solid phase sintering inkjet printing deposition process	0.08 at 298 K	281 $\mu\text{W/m K}^2$ at 298 K	[161]
Fe_xTiS_2	Solid phase sintering Secondary sintering	$\kappa_{ab} = 3.4 \text{ W/mK}$ at 300 K	$\kappa_c = 1.06 \text{ W/m K}$ at 300 K	[162]
$(\text{BiS})_{1-2}(\text{TiS}_2)_2$	Solid phase sintering SPS	0.24 at 700 K	0.69 mW/m K^2 at 700 K	[163]
TiS_2 monolayer	Using first-principle calculations	0.95 at 298 K	5 W/m K^2 at 30 K	[164]
$\text{TiS}_2/\text{hexylamine}$	Solid phase sintering	0.4 at 430 K	1460 $\mu\text{W/m K}^2$ at 430 K	[165]

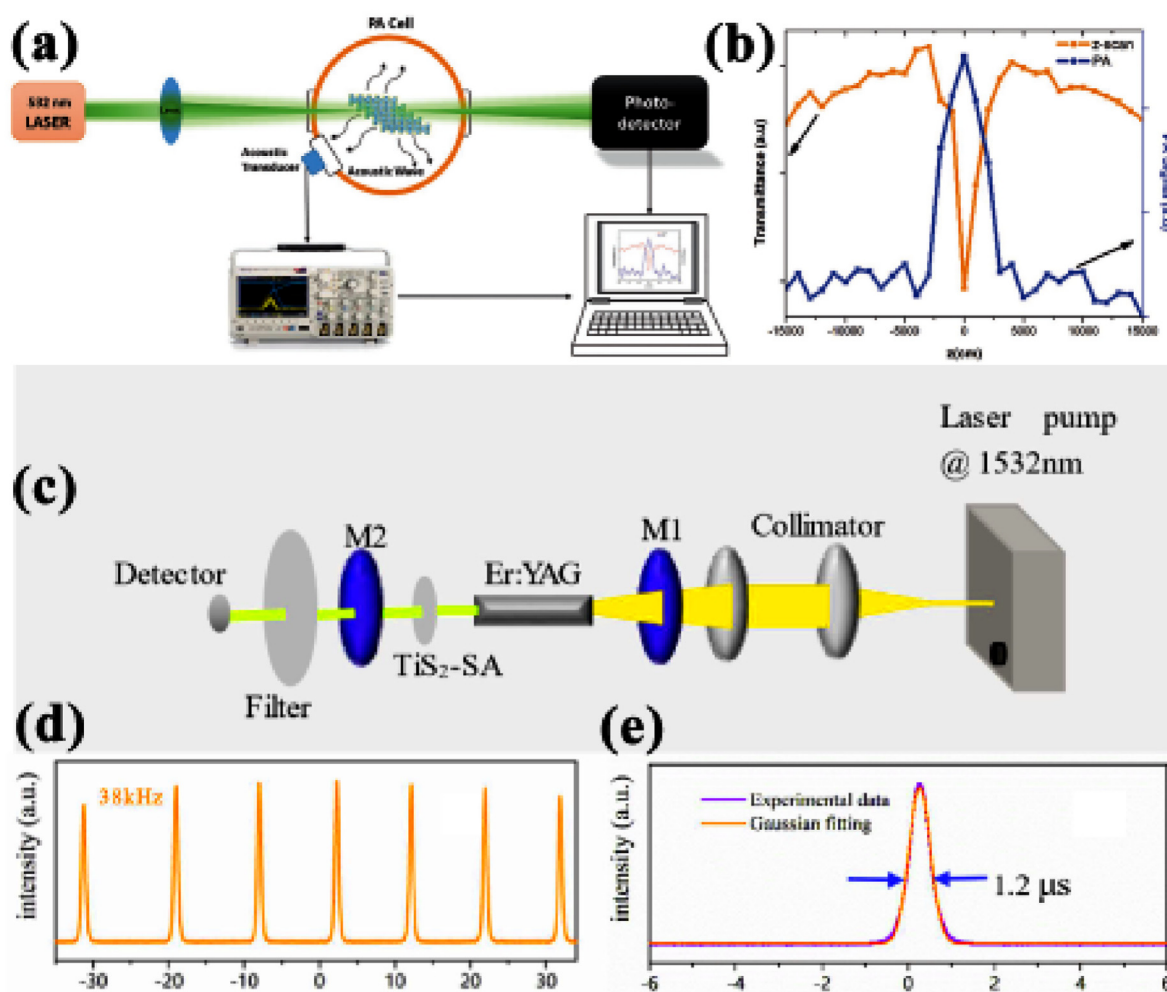


Fig. 9. a) Schematic of the experimental setup used for the OPAC measurements (TiS_2 structure simulated using VESTA software). b) OPAC data of TiS_2 sheets (blue solid line represents the acoustic signal from TiS_2 due to absorption of the incident laser). c) Schematic diagram of passive Q-switched laser using TiS_2 -SA. d) The typical pulse sequence, e) the temporal pulse profile. Ultrafast all-optical switching enabled by TiS_2 switch near optical communication band [94–96].

nonvolatile resistance switching memory device based on a 2D TiS_2 nano film. The manufactured Al/ TiS_2 -PVP/ITO/PET Resistive switching memory device exhibited a good retention time of more than 104s and a cycle durability of 100 cycles. The device's set and reset voltages are less than 2 V. Also, the resistance switch of the device has a very stable bending cycle performance. According to the fitting result of the I–V curve, the dominant conduction mechanism of the low resistance state is the Poole-Frenkel effect, and the high resistance state is mainly controlled by the Shockley equation (Fig. 10e–j).

From the data we have collected, TiS_2 and its composites are most commonly used in thermoelectric devices because of their reasonable material power factor and relatively high thermoelectric properties, as well as its light, mechanically flexible and non-toxic characters meeting the mechanical and health requirements. Benefited by these advantages, TiS_2 nanomaterials may be an excellent candidates for other electronic devices, such as bio-detectors and high-power lasers. Therefore, As summarized in Table 3, the application of TiS_2 nanomaterials and their composites in various types of devices is worth exploring further.

3.3. Catalytic

Catalytic technology occupies a very important position in modern industrial civilization [105–108]. It is also one of the leading technologies in the realization of energy conversion and control of environmental pollution. It also provides a lot of help in promoting the development of

human society and improving the earth's environment [109,110]. With the continuous development of modern human society, the requirements for catalytic technology are becoming more and more stringent. Various research institutions around the world are striving to develop new catalysts with more active sites, larger specific surface area and fewer reaction paths [111–115]. The potential of TiS_2 in the field of catalysis can be reflected in three aspects: specific surface area, mechanical properties and electronic properties. The large surface area associated with the thickness of ultrathin TiS_2 nanosheets is very beneficial for light trapping, mass transfer, and high exposure of surface active sites. Second, the ultra-thin properties of TiS_2 nanosheets significantly shorten the bulk-to-surface charge transfer distance and greatly accelerate the charge transfer process. In addition, the excellent mechanical properties endow the catalyst with durability and thermal conductivity, which are beneficial to facilitate heat diffusion in exothermic reactions. Compared with bulk materials, ultrathin TiS_2 nanosheets are the material of choice for building hierarchical composite catalysts, thus exhibiting excellent performance in the field of catalysis.

3.3.1. Energy catalysis

Hydrogen evolution reaction (HER) [116], oxygen evolution reaction (OER) [117], carbon dioxide reduction reaction (CO₂RR) [118] and oxygen reduction reaction (ORR) [119] are the core of future clean energy conversion technology. The development of efficient catalysts for these catalytic reactions has important implications for clean and

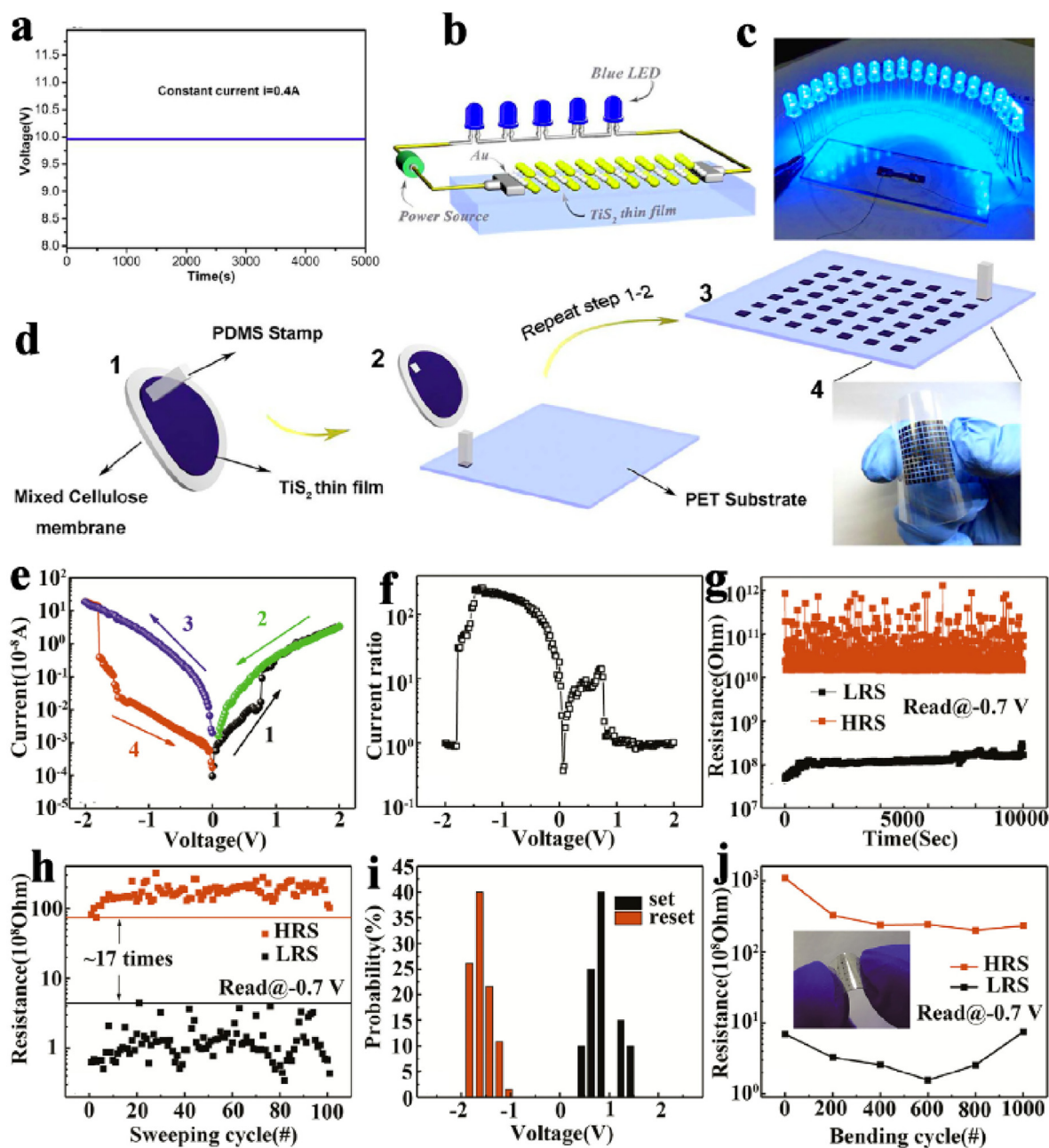


Fig. 10. Excellent high-voltage endurance and improved dry-transfer method for transferrable assembled hydrogenated TiS_2 film. (a) Time-dependent voltage value curve showing the high-voltage endurance with high stability. (b) Schematic illustration of working model for endurance test. (c) Digital photograph of the stability testing setup. (d) Schematic illustration of transfer-printing procedure (1–2) and the designed patterns (3–4). (e) A typical I–V curve of Al/ TiS_2 -PVP/ITO/PET Resistive switching memory devices. (f) The plot of low resistance state/high resistance state current ratio vs. voltage. (g) Retention characteristics under -0.7 V read voltage. (h) Direct current sweeping endurance measured under the same read voltage, -0.7 V. (i) Set and reset voltage distributions among 100 sweeping cycles. (j) High resistance state and low resistance state resistances measured after every 200 repeated bending cycles under -0.7 V read voltage [29,104].

sustainable development. The rich chemical and physical properties of TiS_2 provide opportunities to explore its applications in energy catalysis.

TiS_2 , like other 2D materials, is single-atom and several-atom thick, with unique bonding between layers. It has strong in-plane covalent bonding and weaker van der Waals interactions between layers. This weak van der Waals effect allows it to be easily exfoliated from the bulk material to form ultrathin nanosheets. These ultrathin nanosheets have completely different properties from the bulk material due to their anisotropy. The potential of ultrathin TiS_2 nanosheets for catalytic applications can be summarized in three aspects: large surface area, mechanical properties, and strong conductivity (thermal and electrical). The large specific surface area of the ultrathin TiS_2 nanosheets can provide

more surface active sites; the excellent mechanical properties can provide the persistence of catalysis; and the thermal conductivity can assist the thermal diffusion generated in the reaction. In addition, the ultrathin TiS_2 nanosheets have tunable electronic properties that can better control the catalytic performance; therefore, compared with the bulk materials, the ultrathin TiS_2 nanosheets have better catalytic stability and catalytic activity. The ultrathin TiS_2 nanosheets obtained by different methods also have different catalytic activities. Zeng et al. [120] realized the preparation of single TiS_2 nanomaterials by optimizing the electrochemical lithium intercalation technology, and deposited Pt and Au nanomaterials on single TiS_2 nanomaterials to form composite materials with catalytic function. The composite exhibits good catalytic activity in

Table 3
Summary of TiS₂ and its composites in electronic devices.

Material	Preparation Method	Application	Performance	Ref.
TiS ₂ nanosheet	liquid phase exfoliation	biomolecular detectors	detection limit of 0.01pM	[166]
TiS ₂ nanosheet	Sonication assisted exfoliation	biomolecular detectors	detection limit of 82.7pM	[167]
TiS ₂ nanosheet	chemical Exfoliation	high power lasers	77% nonlinear optical limiting	[94]
TiS ₂ flakes	liquid phase exfoliation	high power lasers	output power of 1.42 W	[95]
multilayer TiS ₂	liquid phase exfoliation	high power lasers	modulation response up to ~145%	[96]
TiS ₂ nanosheet	liquid phase exfoliation	high power lasers	an optical modulation depth of 8.3% at 1560 nm	[168]
Sb ₂ Te ₃ -TiS ₂	Wet mixing	high power lasers	output power of 0.35 W	[169]
TiS ₂ -PEG	Liquid phase reaction	in vivo photoacoustic imaging and photothermal cancer therapy	Complete eradication of tumors in mice	[32]
H _x TiS ₂ nanosheet	chemical Exfoliation and polymerization	Ion detector	detection limit of 0.7 nM	[170]
Al/TiS ₂ PVP/ITO/PET	chemical Exfoliation spin-coated	memory devices	the HRS and the LRS can be kept 104s	[104]
TiS ₂ nanosheet	chemical exfoliation	memory devices	electrical conductivity of 6.76 × 10 ⁴ S/m	[29]
TiS ₂ nanosheet	Liquid phase reaction	Ultra-pulse generation and all-optical threshold devices	signal-to-noise ratio 10.68 dB	[16]

the hydrogen evolution reaction from electrolytic water. Huckaba et al. [121] intercalated CoS between TiS₂ sheets and compared the unmodified TiS₂ material, the water oxidation overpotential was reduced by more than 1.7 V at 10 mA/cm². They believe that exfoliating the interlayer structure of TiS₂ can improve its catalytic activity.

In general, the catalytic properties of TiS₂ depend on the relative pH of the surface atoms, which results from the interaction between cations and anions. A convenient way to modulate this interaction to enhance catalytic activity is to introduce foreign atoms into the crystal lattice of the catalyst (denoted as doping). Replacing the parent atom in the host material with a dopant greatly affects its physicochemical properties. In general, heteroatom lattice doping can regulate the interaction between cations and anions to affect the relative PH value of surface atoms, which helps to improve the catalytic performance of TiS₂. Heteroatom doping also has a great influence on the physical and chemical properties of the material, such as changing the conductivity and carrier density of the material, thereby increasing the charge transfer process. Doping materials with different Fermi levels can be prepared according to different doping modes (n or P doping). Therefore, based on the multiple changes in the physical and chemical properties of TiS₂ nanomaterials, heteroatom doping can adjust the degree of freedom of electrocatalytic activity of metal sites in TiS₂ nanomaterials. Huang et al. [74] modified ultra-thin TiS₂ nanotablets by N, S co-doping and found that Li-S batteries exhibited high capture capacity for lithium polysulfide, as well as significant electrocatalytic activity for reduction of polysulfides and oxidation of lithium sulfide. In addition, they found that TiS₂ can be converted to S-doped TiO₂ with visible photocatalytic activity. Based on this conversion process, Wang et al. [122] successfully synthesized sulfur doped TiO₂ by reacting TiS₂ with water under low-temperature

hydrothermal conditions, and obtained high photocatalytic activity. Lin et al. [123] prepared S-doped TiO₂ with various impurity states by hydrothermal reaction of TiS₂ for the first time in HCl solution. At the same time, TiS₂ in HNO₃ can be converted into N-doped TiO₂, both of which are doped with TiO₂, with good visible light catalytic activity.

Structural defects are believed to be an important cause of low mobility of charge carriers in electrical transport and highly enhanced catalytic activity. First, by creating defects in TiS₂, the electronic structure of the electrocatalyst can be tuned to facilitate the activation of the species involved in the catalytic reaction, thereby enhancing the intrinsic catalytic activity of the electrocatalyst. Second, the low-coordinated and unsaturated Ti sites can be tuned. More active sites created through defect engineering can be exposed at the interface through interface engineering, thereby enhancing the extrinsic catalytic activity of electrocatalysts by increasing the number of active sites. Third, the selectivity (Faraday efficiency) of the catalytic reaction can be improved by adjusting the adsorption energy of the intermediate through the defects of TiS₂. Tisita et al. [124] performed first-principles calculations based on DFT to comprehensively simulate the photocatalytic activity of TiS₂ monolayers that also contain defects. It has a lower overpotential under the influence of vacancy defects. Wu et al. [125] constructed a TiS₂-x/NiS heterostructure with abundant sulfur vacancy defects. Experimental results and theoretical calculations confirm that this non-stoichiometric TiS₂-x/NiS heterostructure accompanied by a large number of sulfur vacancy defects effectively tunes the electronic structures of metallic Ti and Ni atoms, thereby enhancing their HER catalytic kinetics.

3.3.2. Environmental catalysis

Catalytic technology is one of the important means to remove pollutants in the environmental field, especially in the removal of water pollutants. Ultrathin TiS₂ nanosheets show stronger catalytic performance than conventional catalysts due to their advantages of large specific surface area, abundant active sites, unique geometry, and short diffusion paths.

The source of many diseases in the world is related to environmental pollution, which brings great resistance to the healthy life of human society [126]. In particular, water pollution has seriously affected the development of human civilization on the earth [127]. With the rapid development of industry and agriculture, the pollution is becoming more and more serious. A large amount of wastewater containing inorganic and organic compounds discharged into the environment has become a serious threat to the survival of human society, such as the wastewater formed by various chemical dyes in the textile industry. In view of this, how to remove chemical dyes from polluted wastewater is very important. The methods for removing dyes from wastewater include ion exchange, reverse osmosis, chlorination and adsorption. However, these methods are used to transfer pollutants from one medium to another, which has high costs and cannot be permanently removed. Their specific applications are severely limited and do not conform to the concept of sustainable development. Therefore, low-cost and efficient catalytic degradation methods have emerged, which can rapidly and completely oxidize pollutants into fixed products. In recent years, a large number of catalytic materials related to wastewater treatment have been found by researchers and modified by various means to improve their catalytic performance. TiS₂ nanomaterials are widely used as catalysts for wastewater treatment due to their high surface activity, chemical stability, adjustable band gap and large specific surface area. Parvaz et al. [128] successfully synthesized Sb@TiS₂. The photocatalytic degradation of methylene blue dye by nanocomposites was studied. They found that the degradation efficiency of pure TiS₂ nano disk to methylene blue dye was low, but with the increase of antimony weight percentage, the degradation efficiency also increased. Liu et al. [129] firmly fixed TiS₂ nanomaterials on the 2D-C₃N₄ surface by solvothermal method. They found that this can effectively inhibit the recombination of electrons and holes, thereby improving the photocatalytic degradation activity. Moreover, the inherent metal properties of 1 T-TiS₂ also help to improve the

photocatalytic degradation activity. He et al. [130] found that the photocatalytic degradation activity of pure TiS_2 material is much higher than that of some S-doped TiO_2 materials, and the photocatalytic degradation activity of S-doped TiO_2 powder depends on the content of S.

Azo colors are also one of the main industrial pollutants of textiles. These azo colors are usually very stable in nature and will cause very serious environmental pollution if discharged into the environment in large quantities. Researchers have used various physical or chemical methods to extract azo colors from these polluted wastewater, but the effect is not ideal. In recent years, some scientists have achieved remarkable results in the catalytic treatment of azo colors with TiS_2 . For example, Rosy et al. [131] used TiS_2 – TiO_2 nanoparticles as the catalyst and H_2O_2 as the electron acceptor, which effectively prevented the recombination of electron hole pairs, thus improving their photocatalytic activity for the degradation of azo colors, and had good catalytic stability.

4. Summary and outlook

Extensive researches have been carried out on the basic aspects of the synthesis, modification and application of layered TiS_2 . In this review, we have summarized the preparation methods of TiS_2 nanostructured materials, from solid phase, liquid phase, and gas phase synthesis. Among these methods, solid phase and liquid phase reactions are widely used. In addition, we present the progress in application of TiS_2 , including energy storage and conversion, electronic devices and catalytic. The wide applications of nanostructured TiS_2 benefited from its excellent physical/chemical properties such as large specific surface area, adjustable band gap, good visible light absorption characteristics and excellent charge transport characteristics.

Given the current research results, there are many promising research directions need to be explored. Most recent studies have focused on the synthesis of large-area, high-crystallized, ultra-thin TiS_2 nanosheets, however, only a few reports have been conducted for morphology control of TiS_2 . Previous studies reveal that the size and structural orientation of the nanosheets can be adjusted using a suitable substrate (eg, an insulating single crystal substrate, an amorphous SiO_2/Si substrate) [132–135]. Therefore, it is feasible to prepare novel TiS_2 nanomaterials by selecting appropriate substrates and controlling reaction conditions. In addition, transition metals (such as Fe, Co, and Ni) may be doped into the crystal lattice of the TiS_2 to achieve changes in photoelectric properties and catalytic activity [136,137]. From the application of the TiS_2 nanomaterials listed in this paper, the current application of TiS_2 nanomaterials mainly focuses on energy storage and conversion. However, we believe that TiS_2 nanomaterials will become one of the hot materials in the field of electronic devices and catalysis due to their strong visible light absorption and high electron transport properties. Besides, TiS_2 will receive much attention in the field of drug delivery, biotherapy and bio-imaging. There is still plenty of room to explore the application of TiS_2 in interdisciplinary areas. Below we summarize some of the challenges TiS_2 currently faces:

First, one of the biggest challenges is how to synthesize TiS_2 with desired structural features in a highly controllable manner, since the properties and applications of TiS_2 are highly related to all these structural features, such as size, number of layers, doping, defects, vacancies, interlayer spacing, crystallinity and phase. For example, in recent years, the phase of 2D materials has been recognized as one of the key parameters affecting their performance and application performance. However, it is still difficult to precisely design the purity of certain phases, the ratio of different phases, or the phase patterns of 2D materials, a research topic in phase engineering of nanomaterials (PEN). We believe that these characteristics of TiS_2 are very important for its further applications in catalysis and electronics.

Second, the large lateral size and atomic thickness of TiS_2 endow them with many excellent properties, but also inevitably make them stack together during storage and further use, which will greatly diminish their advantages. Therefore, the second challenge is how to prevent TiS_2

nanosheets from stacking or agglomerating during storage and application, thereby avoiding the performance degradation of TiS_2 . Considering that TiS_2 has been widely used, challenges remain for each specific application.

Third, the challenge of TiS_2 in energy storage is how to understand and control the energy storage mechanism and achieve long-term electrochemical stability. Therefore, although TiS_2 has been widely used in solar cells, one of the main challenges in the application of TiS_2 in solar cells is to combine TiS_2 with various functional materials to produce synergistic effects, eliminate non-radiative charge recombination, and have good compatibility with adjacent layers.

Fourth, a major challenge in the application of TiS_2 in the field of photoelectronics is the design and synthesis of narrow band gap TiS_2 semiconductors for the fabrication of infrared photodetectors, especially long-wave infrared photodetectors.

Fifth, although TiS_2 has been proven to be excellent electrocatalysts in many reactions, such as HER and OER, the performance of most TiS_2 -based electrocatalysts decreases rapidly in the long-term stability test, which is one of the main limitations of its practical application in electrocatalysis.

Sixth, a major challenge for TiS_2 in biological applications is to precisely design the structure and composition of TiS_2 for specific biological applications. With excellent sensitivity, selectivity, stability and reproducibility, TiS_2 -based sensor platform has been successfully applied in the fields of environmental monitoring, biochemical analysis, disease diagnosis, food safety, public health security and even homeland security. With the increasing demand for real-world detection, TiS_2 -based sensor platforms are facing challenges.

Seventh, although TiS_2 has a broad application prospects in the field of biomedicine, TiS_2 -related biomedical applications are still facing critical issues of structure/component control for stringent biomedical applications.

Eighth, for TiS_2 in environmental applications, how to reduce the interference during operation, such as expansion, dirt and degradation, in order to maintain the long-term stability of TiS_2 in practical applications.

Declaration of competing interest

The authors declare that they have no known competing financial interests or personal relationships that could have appeared to influence the work reported in this paper.

Acknowledgements

This work was supported by National Natural Science Foundation of China Project [No. 51827901, 22109101, 62205212], Program for Guang Dong Introducing Innovative and Entrepreneurial Teams [No. 2019ZT08G315], General program of China Postdoctoral Science Foundation [No. 2022M722179], the Natural Science Foundation of Guangdong Province [No. 2020A1515010550] and the Shenzhen Basic Research Program (No. JCYJ20210324093008021).

References

- [1] A.K. Geim, K.S. Novoselov, *The rise of graphene*, in: *Nanoscience and Technology*, Co-Published with Macmillan Publishers Ltd, UK, 2009, p. 11.
- [2] M. Ge, C. Cao, J. Huang, S. Li, Z. Chen, K.-Q. Zhang, S. Al-Deyab, Y. Lai, *A review of one-dimensional TiO_2 nanostructured materials for environmental and energy applications*, *J. Mater. Chem.* 4 (2016) 6772.
- [3] M. Chhowalla, H.S. Shin, G. Eda, L.-J. Li, K.P. Loh, H. Zhang, *The chemistry of two-dimensional layered transition metal dichalcogenide nanosheets*, *Nat. Chem.* 5 (2013) 263.
- [4] X. Zhang, H. Cheng, H. Zhang, *Recent progress in the preparation, assembly, transformation, and applications of layer-structured nanodisks beyond graphene*, *Adv. Mater.* 29 (2017), 1701704.
- [5] G.L. Holleck, J.R. Driscoll, *Transition metal sulfides as cathodes for secondary lithium batteries—II. titanium sulfides*, *Electrochim. Acta* 22 (1977) 647.

- [6] A. Chaturvedi, E. Edison, N. Arun, P. Hu, C. Kloc, V. Aravindan, S. Madhavi, Two dimensional TiS₂ as a promising insertion anode for Na-ion battery, *ChemistrySelect* 3 (2018) 524.
- [7] M. Minakshi, A. Pandey, M. Blackford, M. Ionescu, Effect of TiS₂ additive on LiMnPO₄ cathode in aqueous solutions, *Energy Fuels* 24 (2010) 6193.
- [8] L. Wang, J. Zou, S. Chen, G. Zhou, J. Bai, P. Gao, Y. Wang, X. Yu, J. Li, Y.-S. Hu, H. Li, TiS₂ as a high performance potassium ion battery cathode in ether-based electrolyte, *Energy Storage Mater.* 12 (2018) 216.
- [9] C.M. Fang, R.A. de Groot, C. Haas, Bulk and surface electronic structure of 1T–TiS₂ and 1T–TiSe₂, *Phys. Rev. B* 56 (1997) 4455.
- [10] P.C. Sherrell, K. Sharda, C. Grotta, J. Ranalli, M.S. Sokolikova, F.M. Pesci, P. Palczynski, V.L. Bemmer, C. Mattevi, Thickness-dependent characterization of chemically exfoliated TiS₂ nanosheets, *ACS Omega* 3 (2018) 8655.
- [11] A. Stoliaroff, S. Jobic, C. Latouche, Optoelectronic properties of TiS₂: a never ended story tackled by density functional theory and many-body methods, *Inorg. Chem.* 58 (2019) 1949.
- [12] A. Chaturvedi, P. Hu, V. Aravindan, C. Kloc, S. Madhavi, Unveiling two-dimensional TiS₂ as an insertion host for the construction of high energy Li-ion capacitors, *J. Mater. Chem.* 5 (2017) 9177.
- [13] M.R. Ryzhikov, V.A. Slepikov, S.G. Kozlova, S.P. Gabuda, Evolution of chemical bonding and electron density rearrangements during D3h → D3d reaction in monolayered TiS₂: a QTAIM and ELF study, *J. Comput. Chem.* 35 (2014) 1641.
- [14] A. Samad, A. Shafique, Y.-H. Shin, Adsorption and diffusion of mono, di, and trivalent ions on two-dimensional TiS₂, *Nanotechnology* 28 (2017), 175401.
- [15] T. Lorenz, D. Teich, J.-O. Joswig, G. Seifert, Theoretical study of the mechanical behavior of individual TiS₂ and MoS₂ nanotubes, *J. Phys. Chem. C* 116 (2012), 11714.
- [16] Y. Ge, Z. Zhu, Y. Xu, Y. Chen, S. Chen, Z. Liang, Y. Song, Y. Zou, H. Zeng, S. Xu, H. Zhang, D. Fan, Broadband nonlinear photoresponse of 2D TiS₂ for ultrashort pulse generation and all-optical thresholding devices, *Adv. Opt. Mater.* 6 (2018), 1701166.
- [17] Z. Zhu, Y. Zou, W. Hu, Y. Li, Y. Gu, B. Cao, N. Guo, L. Wang, J. Song, S. Zhang, H. Gu, H. Zeng, Near-infrared plasmonic 2D semimetals for applications in communication and biology, *Adv. Funct. Mater.* 26 (2016) 1793.
- [18] B. Liu, J. Yang, C. Liu, T. Hu, Y. Han, C. Gao, The ground electronic state of TiS₂: experimental and theoretical studies, *Phys. Status Solidi C* 8 (2011) 1683.
- [19] C.S. Cucinotta, K. Dolui, H. Pettersson, Q.M. Ramasse, E. Long, S.E. O'Brian, V. Nicolosi, S. Sanvito, Electronic properties and chemical reactivity of TiS₂ nanoflakes, *J. Phys. Chem. C* 119 (2015), 15707.
- [20] F.R. Shepherd, P.M. Williams, Photoemission studies of the band structures of transition metal dichalcogenides. I. Groups IVA and IVB, *J. Phys. C Solid State Phys.* 7 (1974) 4416.
- [21] S.C. Bayliss, W.Y. Liang, Reflectivity, joint density of states and band structure of group IVb transition-metal dichalcogenides, *J. Phys. C Solid State Phys.* 18 (1985) 3327.
- [22] Z. Yang, Y. Jiang, W. Zhang, Y. Ding, Y. Jiang, J. Yin, P. Zhang, H. Luo, Solid-state, low-cost, and green synthesis and robust photochemical hydrogen evolution performance of ternary TiO₂/mgTiO₃/C photocatalysts, *iScience* 14 (2019) 15.
- [23] S.S. Tamhankar, L.K. Doraiswamy, Analysis of solid-solid reactions: a review, *AIChE J.* 25 (1979) 561.
- [24] M. Malekshahi Byranvand, A. Nemat Kharat, L. Fathollahi, Z. Malekshahi Beiranvand, A review on synthesis of nano-TiO₂ via different methods, *J. Nanostruct* 3 (2013) 1.
- [25] Z. Yang, C. Deng, Y. Ding, H. Luo, J. Yin, Y. Jiang, P. Zhang, Y. Jiang, Eco-friendly and effective strategy to synthesize ZnO/Ag₂O heterostructures and its excellent photocatalytic property under visible light, *J. Solid State Chem.* 268 (2018) 83.
- [26] E.A. Meulenkaamp, Synthesis and growth of ZnO nanoparticles, *J. Phys. Chem. B* 102 (1998) 5566.
- [27] J. Theerthagiri, R.A. Senthil, B. Senthilkumar, A. Reddy Polu, J. Madhavan, M. Ashokkumar, Recent advances in MoS₂ nanostructured materials for energy and environmental applications – a review, *J. Solid State Chem.* 252 (2017) 43.
- [28] C.G. Hawkins, L. Whittaker-Brooks, Vertically oriented TiS₂-x nanobelt arrays as binder- and carbon-free intercalation electrodes for Li- and Na-based energy storage devices, *J. Mater. Chem.* 6 (2018), 21949.
- [29] C. Lin, X. Zhu, J. Feng, C. Wu, S. Hu, J. Peng, Y. Guo, L. Peng, J. Zhao, J. Huang, J. Yang, Y. Xie, Hydrogen-incorporated TiS₂ ultrathin nanosheets with ultrahigh conductivity for stamp-transferable electrodes, *J. Appl. Comput. Sci.* 135 (2013) 5144.
- [30] X. Sun, P. Bonnick, L.F. Nazar, Layered TiS₂ positive electrode for Mg batteries, *ACS Energy Lett.* 1 (2016) 297.
- [31] H. Tao, M. Zhou, R. Wang, K. Wang, S. Cheng, K. Jiang, TiS₂ as an advanced conversion electrode for sodium-ion batteries with ultra-high capacity and long-cycle life, *Adv. Sci.* 5 (2018), 1801021.
- [32] X. Qian, S. Shen, T. Liu, L. Cheng, Z. Liu, Two-dimensional TiS₂ nanosheets for in vivo photoacoustic imaging and photothermal cancer therapy, *Nanoscale* 7 (2015) 6380.
- [33] Y. Zhao, W. Cai, Y. Fang, H. Ao, Y. Zhu, Y. Qian, Sulfur-deficient TiS₂-x for promoted polysulfide redox conversion in lithium-sulfur batteries, *Chemelectrochem* 6 (2019) 2231.
- [34] C.G. Hawkins, L. Whittaker-Brooks, Controlling sulfur vacancies in TiS₂-x cathode insertion hosts via the conversion of TiS₃ nanobelts for energy-storage applications, *ACS Appl. Nano Mater.* 1 (2018) 851.
- [35] H. Ma, Z. Tao, F. Gao, J. Chen, H. Yuan, Synthesis, characterization and hydrogen storage capacity of MS₂ (M = Mo, Ti) nanotubes, *Front. Chem. China* 1 (2006) 260.
- [36] Z. Lei, S. Xu, J. Wan, P. Wu, Facile preparation and multifunctional applications of boron nitride quantum dots, *Nanoscale* 7 (2015), 18902.
- [37] H. Li, R.Y. Tay, S.H. Tsang, X. Zhen, E.H.T. Teo, Controllable synthesis of highly luminescent boron nitride quantum dots, *Small* 11 (2015) 6491.
- [38] M. Nasilowski, B. Mahler, E. Lhuillier, S. Ithurria, B. Dubertret, Two-dimensional colloidal nanocrystals, *Chem. Rev.* 116 (2016), 10934.
- [39] T.-H. Yang, H.-C. Peng, S. Zhou, C.-T. Lee, S. Bao, Y.-H. Lee, J.-M. Wu, Y. Xia, Toward a quantitative understanding of the reduction pathways of a salt precursor in the synthesis of metal nanocrystals, *Nano Lett.* 17 (2017) 334.
- [40] G. Singh, B.H. McDonagh, S. Hak, D. Peddis, S. Bandopadhyay, I. Sandvig, A. Sandvig, W.R. Glomm, Synthesis of gadolinium oxide nanodisks and gadolinium doped iron oxide nanoparticles for MR contrast agents, *J. Mater. Chem. B* 5 (2017) 418.
- [41] A. Wolcott, T.R. Kuykendall, W. Chen, S. Chen, J.Z. Zhang, Synthesis and characterization of ultrathin WO₃ nanodisks utilizing long-chain poly(ethylene glycol), *J. Phys. Chem. B* 110 (2006), 25288.
- [42] S. Ithurria, G. Bousquet, B. Dubertret, Continuous transition from 3D to 1D confinement observed during the formation of CdSe nanoplatelets, *J. Appl. Comput. Sci.* 133 (2011) 3070.
- [43] S. Ithurria, B. Dubertret, Quasi 2D colloidal CdSe platelets with thicknesses controlled at the atomic level, *J. Appl. Comput. Sci.* 130 (2008), 16504.
- [44] E. Lhuillier, S. Pedetti, S. Ithurria, B. Nadal, H. Heuclin, B. Dubertret, Two-dimensional colloidal metal chalcogenides semiconductor: synthesis, spectroscopy, and applications, *Accounts Chem. Res.* 48 (2015) 22.
- [45] C. Bouet, M.D. Tessier, S. Ithurria, B. Mahler, B. Nadal, B. Dubertret, Flat colloidal semiconductor nanoplatelets, *Chem. Mater.* 25 (2013) 1262.
- [46] A.J. Huckaba, S. Gharibzadeh, M. Ralaivisoa, C. Roldán-Carmona, N. Mohammadian, G. Grancini, Y. Lee, P. Amsalem, E.J. Plichta, N. Koch, A. Moshahi, M.K. Nazeeruddin, Low-cost TiS₂ as hole-transport material for perovskite solar cells, *Small Methods* 1 (2017), 1700250.
- [47] Y. Liu, H. Wang, L. Cheng, N. Han, F. Zhao, P. Li, C. Jin, Y. Li, TiS₂ nanoplates: a high-rate and stable electrode material for sodium ion batteries, *Nano Energy* 20 (2016) 168.
- [48] K.H. Park, J. Choi, H.J. Kim, D.-H. Oh, J.R. Ahn, S.U. Son, Unstable single-layered colloidal TiS₂ nanodisks, *Small* 4 (2008) 945.
- [49] J. Chen, Z.-L. Tao, S.-L. Li, Lithium intercalation in open-ended TiS₂ nanotubes, *Angew. Chem. Int. Ed.* 42 (2003) 2147.
- [50] M. Tan, Z. Wang, J. Peng, X. Jin, Facile synthesis of large and thin TiS₂ sheets via a gas/molten salt interface reaction, *J. Am. Ceram. Soc.* 98 (2015) 1423.
- [51] D.Y. Oh, Y.E. Choi, D.H. Kim, Y.-G. Lee, B.-S. Kim, J. Park, H. Sohn, Y.S. Jung, All-solid-state lithium-ion batteries with TiS₂ nanosheets and sulphide solid electrolytes, *J. Mater. Chem.* 4 (2016), 10329.
- [52] A. Margolin, R. Popovitz-Biro, A. Abu-Yaron, L. Rapoport, R. Tenne, Inorganic fullerene-like nanoparticles of TiS₂, *Chem. Phys. Lett.* 411 (2005) 162.
- [53] Y. Zhang, Z. Li, H. Jia, X. Luo, J. Xu, X. Zhang, D. Yu, TiS₂ whisker growth by a simple vapor-deposition method, *J. Cryst. Growth* 293 (2006) 124.
- [54] B. Tian, W. Tang, K. Leng, Z. Chen, S.J.R. Tan, C. Peng, G.-H. Ning, W. Fu, C. Su, G.W. Zheng, K.P. Loh, Phase transformations in TiS₂ during K intercalation, *ACS Energy Lett.* 2 (2017) 1835.
- [55] B. Han, S. Chen, J. Zou, R. Shao, Z. Dou, C. Yang, X. Ma, J. Lu, K. Liu, D. Yu, L. Wang, H. Wang, P. Gao, Tracking sodium migration in TiS₂ using in situ TEM, *Nanoscale* 11 (2019) 7474.
- [56] T.A. Yersak, J.E. Trevey, S.-H. Lee, In situ lithiation of TiS₂ enabled by spontaneous decomposition of Li₃N, *J. Power Sources* 196 (2011) 9830.
- [57] M. Ge, C. Cao, J. Huang, S. Li, Z. Chen, K.-Q. Zhang, S.S. Al-Deyab, Y. Lai, A review of one-dimensional TiO₂ nanostructured materials for environmental and energy applications, *J. Mater. Chem.* 4 (2016) 6772.
- [58] Y. Zhao, Y. Zhang, Z. Yang, Y. Yan, K. Sun, Synthesis of MoS₂ and MoO₂ for their applications in H₂ generation and lithium ion batteries: a review, *Sci. Technol. Adv. Mater.* 14 (2013), 043501.
- [59] A. Unemoto, T. Ikeshoji, S. Yasaku, M. Matsuo, V. Stavila, T.J. Udovic, S.-i. Orimo, Stable interface formation between TiS₂ and LiBH₄ in bulk-type all-solid-state lithium batteries, *Chem. Mater.* 27 (2015) 5407.
- [60] M. Minakshi, P. Singh, D.R.G. Mitchell, T.B. Issa, K. Prince, A study of lithium insertion into MnO₂ containing TiS₂ additive a battery material in aqueous LiOH solution, *Electrochim. Acta* 52 (2007) 7007.
- [61] M. Shahjalal, P.K. Roy, T. Shams, A. Fly, J.I. Chowdhury, M.R. Ahmed, K. Liu, A review on second-life of Li-ion batteries: prospects, challenges, and issues, *Energy* 241 (2022), 122881.
- [62] J. Trevey, C. Stoldt, S.-H. Lee, TiS₂/S composite materials for all-solid-state lithium batteries, *Meet. Abstr. MA2010-02* (2010) 1095.
- [63] J.E. Trevey, C.R. Stoldt, S.-H. Lee, High power nanocomposite TiS₂ cathodes for all-solid-state lithium batteries, *J. Electrochem. Soc.* 158 (2011) A1282.
- [64] Y.-E. Huang, W. Lin, C. Shi, L. Li, K. Fan, X.-Y. Huang, X. Wu, K.-Z. Du, Misfit layer SnTiS₃: an assemble-free van der Waals heterostructure SnS/TiS₂ for lithium ion battery anode, *J. Power Sources* 494 (2021), 229712.
- [65] J.Y. Kim, J. Park, S.H. Kang, S. Jung, D.O. Shin, M.J. Lee, J. Oh, K.-M. Kim, J. Zausch, Y.-G. Lee, Y.M. Lee, Revisiting TiS₂ as a diffusion-dependent cathode with promising energy density for all-solid-state lithium secondary batteries, *Energy Storage Mater.* 41 (2021) 289.
- [66] L. Zhang, D. Sun, J. Kang, H.-T. Wang, S.-H. Hsieh, W.-F. Pong, H.A. Bechtel, J. Feng, L.-W. Wang, E.J. Cairns, J. Guo, Tracking the chemical and structural evolution of the TiS₂ electrode in the lithium-ion cell using operando X-ray absorption spectroscopy, *Nano Lett.* 18 (2018) 4506.

- [67] W. Sun, L. Suo, F. Wang, N. Eidson, C. Yang, F. Han, Z. Ma, T. Gao, M. Zhu, C. Wang, "Water-in-Salt" electrolyte enabled LiMn₂O₄/TiS₂ Lithium-ion batteries, *Electrochem. Commun.* 82 (2017) 71.
- [68] S.-H. Chung, L. Luo, A. Manthiram, TiS₂-Polysulfide hybrid cathode with high sulfur loading and low electrolyte consumption for lithium-sulfur batteries, *ACS Energy Lett.* 3 (2018) 568.
- [69] K. Sun, M. Fu, Z. Xie, D. Su, H. Zhong, J. Bai, E. Dooryhee, H. Gan, Improvement of Li-S battery electrochemical performance with 2D TiS₂ additive, *Electrochim. Acta* 292 (2018) 779.
- [70] W. Zhao, L.-C. Xu, R. Li, Y. Guo, Z. Yang, R. Liu, X. Li, Enhance the anchoring and catalytic performance of lithium-sulfur batteries for lithium polysulfide by predicted TiS₂ monolayer, *Mater. Today Commun.* 30 (2022), 103196.
- [71] Y. Yao, S. Wang, X. Jia, J. Yang, Y. Li, J. Liao, H. Song, Freestanding sandwich-like hierarchically TiS₂-TiO₂/Mxene bi-functional interlayer for stable Li-S batteries, *Carbon* 188 (2022) 533.
- [72] A. Garsuch, S. Herzog, L. Montag, A. Krebs, K. Leitner, Performance of blended TiS₂/sulfur/carbon cathodes in lithium-sulfur cells, *ECS Electrochem. Lett.* 1 (2012) A24.
- [73] S.-H. Chung, A. Manthiram, A Li₂S-TiS₂-Electrolyte composite for stable Li₂S-based lithium-sulfur batteries, *Adv. Energy Mater.* 9 (2019), 1901397.
- [74] X. Huang, J. Tang, B. Luo, R. Knibbe, T. Lin, H. Hu, M. Rana, Y. Hu, X. Zhu, Q. Gu, D. Wang, L. Wang, Sandwich-like ultrathin TiS₂ nanosheets confined within N, S codoped porous carbon as an effective polysulfide promoter in lithium-sulfur batteries, *Adv. Energy Mater.* 9 (2019), 1901872.
- [75] Z. Hu, Z. Tai, Q. Liu, S.-W. Wang, H. Jin, S. Wang, W. Lai, M. Chen, L. Li, L. Chen, Z. Tao, S.-L. Chou, Ultrathin 2D TiS₂ nanosheets for high capacity and long-life sodium ion batteries, *Adv. Energy Mater.* 9 (2019), 1803210.
- [76] D. Chodvadiya, U. Jha, P. Śpięwak, K.J. Kurzydłowski, P.K. Jha, Potential anodic application of 2D h-AlC for Li and Na-ions batteries, *Appl. Surf. Sci.* 593 (2022), 153424.
- [77] A. Chaturvedi, P. Hu, Y. Long, C. Kloc, S. Madhavi, V. Aravindan, High power Na-ion capacitor with TiS₂ as insertion host, *Scripta Mater.* 161 (2019) 54.
- [78] J. Tang, X. Huang, T. Lin, T. Qiu, H. Huang, X. Zhu, Q. Gu, B. Luo, L. Wang, MXene derived TiS₂ nanosheets for high-rate and long-life sodium-ion capacitors, *Energy Storage Mater.* 26 (2020) 550.
- [79] T. Liu, X. Zhang, M. Xia, H. Yu, N. Peng, C. Jiang, M. Shui, Y. Xie, T.-F. Yi, J. Shu, Functional cation defects engineering in TiS₂ for high-stability anode, *Nano Energy* 67 (2020), 104295.
- [80] H.D. Yoo, Y. Liang, Y. Li, Y. Yao, High areal capacity hybrid magnesium-lithium-ion battery with 99.9% coulombic efficiency for large-scale energy storage, *ACS Appl. Mater. Interfaces* 7 (2015) 7001.
- [81] Z.-L. Tao, L.-N. Xu, X.-L. Gou, J. Chen, H.-T. Yuan, TiS₂ 2D nanotubes as the cathode materials of Mg-ion batteries, *Chem. Commun.* (2004) 2080.
- [82] W. Lee, H. Son, T. Kim, H. Kim, S. Kim, D. Chan Lim, Y. Kim, Pronounced thickness effect of permanent charge-introduced branched poly(ethylene imine) surface-modifying layers in polymer:nonfullerene solar cells, *Appl. Surf. Sci.* (2022), 155249.
- [83] Y. Lei, D. Zhang, J. Wu, H. Guo, X. Li, Y. Fang, D. Xie, Y. Lin, Enhancing the photoinduced hole transport in solid state quantum-dots solar cells: the case of CdSe, *Appl. Surf. Sci.* 600 (2022), 154136.
- [84] Y. Lei, Y. Li, Z. Jin, Photon energy loss and management in perovskite solar cells, *Energy Rev.* 1 (2022), 100003.
- [85] N. Alias, A. Ali Umar, N.A.A. Malek, K. Liu, X. Li, N.A. Abdullah, M.M. Rosli, M.Y. Abd Rahman, Z. Shi, X. Zhang, H. Zhang, F. Liu, J. Wang, Y. Zhan, Photoelectrical dynamics uplift in perovskite solar cells by atoms thick 2D TiS₂ layer passivation of TiO₂ nanograss electron transport layer, *ACS Appl. Mater. Interfaces* 13 (2021) 3051.
- [86] G. Yin, H. Zhao, J. Feng, J. Sun, J. Yan, Z. Liu, S. Lin, S. Liu, Low-temperature and facile solution-processed two-dimensional TiS₂ as an effective electron transport layer for UV-stable planar perovskite solar cells, *J. Mater. Chem.* 6 (2018) 9132.
- [87] P. Huang, L. Yuan, K. Zhang, Q. Chen, Y. Zhou, B. Song, Y. Li, Room-temperature and aqueous solution-processed two-dimensional TiS₂ as an electron transport layer for highly efficient and stable planar n-i-p perovskite solar cells, *ACS Appl. Mater. Interfaces* 10 (2018), 14796.
- [88] M. Lickleder, G. Cha, R. Hahn, P. Schmuki, Ordered nanotubular titanium disulfide (TiS₂) structures: synthesis and use as counter electrodes in dye sensitized solar cells (DSSCs), *J. Electrochem. Soc.* 166 (2019) H3009.
- [89] Z. Zeng, Z. Yin, X. Huang, H. Li, Q. He, G. Lu, F. Boey, H. Zhang, Single-layer semiconducting nanosheets: high-yield preparation and device fabrication, *Angew. Chem. Int. Ed.* 50 (2011), 11093.
- [90] W. Fang, H. Wei, X. Xiao, Y. Chen, K. Kuang, M. Li, Y. He, XTiO (X = K, Rb, Cs): novel 2D semiconductors with high electron mobilities, ultra-low lattice thermal conductivities and high thermoelectric figures of merit at room temperature, *Appl. Surf. Sci.* 599 (2022), 153924.
- [91] N. Nandihalli, Imprints of interfaces in thermoelectric materials, *CRIT REV SOLID STATE* (2022) 1.
- [92] R. Tian, C. Wan, Y. Wang, Q. Wei, T. Ishida, A. Yamamoto, A. Tsuruta, W. Shin, S. Li, K. Koumoto, A solution-processed TiS₂/organic hybrid superlattice film towards flexible thermoelectric devices, *J. Mater. Chem.* 5 (2017) 564.
- [93] C. Wan, X. Gu, F. Dang, T. Itoh, Y. Wang, H. Sasaki, M. Kondo, K. Koga, K. Yabuki, G.J. Snyder, R. Yang, K. Koumoto, Flexible n-type thermoelectric materials by organic intercalation of layered transition metal dichalcogenide TiS₂, *Nat. Mater.* 14 (2015) 622.
- [94] S.J. Varma, J. Kumar, Y. Liu, K. Layne, J. Wu, C. Liang, Y. Nakanishi, A. Aliyan, W. Yang, P.M. Ajayan, J. Thomas, 2D TiS₂ layers: a superior nonlinear optical limiting material, *Adv. Opt. Mater.* 5 (2017), 1700713.
- [95] G. Li, C. Wu, Z. Yan, S. Zhang, J. Su, T. Li, TiS₂ as a novel saturable absorber for a 1645 nm passively Q-switched laser, *Laser Phys.* 29 (2019), 055801.
- [96] X. Tian, R. Wei, M. Liu, C. Zhu, Z. Luo, F. Wang, J. Qiu, Ultrafast saturable absorption in TiS₂ induced by non-equilibrium electrons and the generation of a femtosecond mode-locked laser, *Nanoscale* 10 (2018) 9608.
- [97] R. Maleki, A. Miri Jahromi, S. Mohaghegh, S. Rezvantaleb, M. Khedri, L. Tayebi, A molecular investigation of urea and creatinine removal in the wearable dialysis device using Two-Dimensional materials, *Appl. Surf. Sci.* 566 (2021), 150629.
- [98] H. Jiang, J. Chen, Y. Shi, P. Chen, X. Tang, W. Jiang, Z. Zou, G. Wu, A wearable All-Solid-State supercapacitor with extremely high stability based on 2D Co-HCF/GO, *Appl. Surf. Sci.* 586 (2022), 152739.
- [99] M.M. Quazi, M. Ishak, M.A. Fazal, A. Arslan, S. Rubaiee, M.H. Aiman, A. Qaban, F. Yusof, T. Sultan, M.M. Ali, S.M. Manladan, A comprehensive assessment of laser welding of biomedical devices and implant materials: recent research, development and applications, *CRIT REV SOLID STATE* 46 (2021) 109.
- [100] M. Li, K. Chang, W. Zhong, C. Xiang, W. Wang, Q. Liu, K. Liu, Y. Wang, Z. Lu, D. Wang, A highly stretchable, breathable and thermoregulatory electronic skin based on the polyolefin elastomer nanofiber membrane, *Appl. Surf. Sci.* 486 (2019) 249.
- [101] A. Basu, Chapter 7 - smart electronic yarns and wearable fabrics for human biomonitoring, in: A. Ehrmann, T.A. Nguyen, P. Nguyen Tri (Eds.), *Nanosensors and Nanodevices for Smart Multifunctional Textiles*, Elsevier, 2021, p. 109.
- [102] J.L. MacManus-Driscoll, S.C. Wimbush, Processing and application of high-temperature superconducting coated conductors, *Nat. Rev. Mater.* 6 (2021) 587.
- [103] J.-L. Meng, T.-Y. Wang, Z.-Y. He, L. Chen, H. Zhu, L. Ji, Q.-Q. Sun, S.-J. Ding, W.-Z. Bao, P. Zhou, D.W. Zhang, Flexible boron nitride-based memristor for in situ digital and analogue neuromorphic computing applications, *Mater. Horiz.* 8 (2021) 538.
- [104] D. Lyu, C. Hu, Y. Jiang, N. Bai, Q. Wang, D. He, J. Qi, Y. Li, Resistive switching behavior and mechanism of room-temperature-fabricated flexible Al/TiS₂-PVP/ITO/PET memory devices, *Curr. Appl. Phys.* 19 (2019) 458.
- [105] M. Misono, N. Nojiri, Recent progress in catalytic technology in Japan, *Appl. Catal.* 64 (1990) 1.
- [106] J.N. Armor, New catalytic technology commercialized in the USA during the 1980s, *Appl. Catal.* 78 (1991) 141.
- [107] J.N. Armor, New catalytic technology commercialized in the USA during the 1990s, *Appl Catal A-gen* 222 (2001) 407.
- [108] J. Tang, T. Liu, S. Miao, Y. Cho, Emerging energy harvesting technology for electro/photo-catalytic water splitting application, in: *Catalysts*, 2021.
- [109] A. Nizhou, B. Stanmore, N. Lyczko, D.P. Minh, The catalytic effect of inherent and adsorbed metals on the fast/flash pyrolysis of biomass: a review, *Energy* 170 (2019) 326.
- [110] Y. Guo, M. Wen, G. Li, T. An, Recent advances in VOC elimination by catalytic oxidation technology onto various nanoparticles catalysts: a critical review, *Appl. Catal. B Environ.* 281 (2021), 119447.
- [111] X. Yang, S. Wang, Y. He, Review of catalytic reforming for hydrogen production in a membrane-assisted fluidized bed reactor, *Renew. Sustain. Energy Rev.* 154 (2022), 111832.
- [112] Y. Zhao, G.I.N. Waterhouse, G. Chen, X. Xiong, L.-Z. Wu, C.-H. Tung, T. Zhang, Two-dimensional-related catalytic materials for solar-driven conversion of CO_x into valuable chemical feedstocks, *Chem. Soc. Rev.* 48 (2019) 1972.
- [113] J. Deng, D. Deng, X. Bao, Robust catalysis on 2D materials encapsulating metals: concept, application, and perspective, *Adv. Mater.* 29 (2017), 1606967.
- [114] Q. Fu, J. Han, X. Wang, P. Xu, T. Yao, J. Zhong, W. Zhong, S. Liu, T. Gao, Z. Zhang, L. Xu, B. Song, 2D transition metal dichalcogenides: design, modulation, and challenges in electrocatalysis, *Adv. Mater.* 33 (2021), 1907818.
- [115] Y. Zhou, Z. Wang, L. Huang, S. Zaman, K. Lei, T. Yue, Z.-a. Li, B. You, B.Y. Xia, Engineering 2D photocatalysts toward carbon dioxide reduction, *Adv. Energy Mater.* 11 (2021), 2003159.
- [116] Y. Jiang, H. Pang, X. Sun, Z. Yang, Y. Ding, Z. Liu, P. Zhang, TiO₂ nanobelts with ultra-thin mixed C/SiO_x coating as high-performance photo/photoelectrochemical hydrogen evolution materials, *Appl. Surf. Sci.* 537 (2021), 147861.
- [117] F.-Y. Chen, Z.-Y. Wu, Z. Adler, H. Wang, Stability challenges of electrocatalytic oxygen evolution reaction: from mechanistic understanding to reactor design, *Joule* 5 (2021) 1704.
- [118] C. Kim, F. Dionigi, V. Beermann, X. Wang, T. Möller, P. Strasser, Alloy nanocatalysts for the electrochemical oxygen reduction (ORR) and the direct electrochemical carbon dioxide reduction reaction (CO₂RR), *Adv. Mater.* 31 (2019), 1805617.
- [119] X. Tian, X.F. Lu, B.Y. Xia, X.W. Lou, Advanced electrocatalysts for the oxygen reduction reaction in energy conversion technologies, *Joule* 4 (2020) 45.
- [120] Z. Zeng, C. Tan, X. Huang, S. Bao, H. Zhang, Growth of noble metal nanoparticles on single-layer TiS₂ and TaS₂ nanosheets for hydrogen evolution reaction, *Energy Environ. Sci.* 7 (2014) 797.
- [121] A.J. Huckaba, M. Ralaiaarisoa, K.T. Cho, E. Oveisi, N. Koch, M.K. Nazeeruddin, Intercalation makes the difference with TiS₂: boosting electrocatalytic water oxidation activity through Co intercalation, *J. Mater. Res.* 33 (2018) 528.
- [122] F. Wang, F. Li, L. Zhang, H. Zeng, Y. Sun, S. Zhang, X. Xu, S-TiO₂ with enhanced visible-light photocatalytic activity derived from TiS₂ in deionized water, *Mater. Res. Bull.* 87 (2017) 20.
- [123] Y.-C. Lin, T.-E. Chien, P.-C. Lai, Y.-H. Chiang, K.-L. Li, J.-L. Lin, TiS₂ transformation into S-doped and N-doped TiO₂ with visible-light catalytic activity, *Appl. Surf. Sci.* 359 (2015) 1.
- [124] T. Das, S. Chakraborty, R. Ahuja, G.P. Das, TiS₂ monolayer as an emerging ultrathin bifunctional catalyst: influence of defects and functionalization, *ChemPhysChem* 20 (2019) 608.

- [125] J. Wu, W. Zhong, C. Yang, W. Xu, R. Zhao, H. Xiang, Q. Zhang, X. Li, N. Yang, Sulfur-vacancy rich nonstoichiometric TiS₂-x/NiS heterostructures for superior universal hydrogen evolution, *Appl. Catal. B Environ.* 310 (2022), 121332.
- [126] C. Long, Z. Jiang, J. Shanguan, T. Qing, P. Zhang, B. Feng, Applications of carbon dots in environmental pollution control: a review, *Chem. Eng. J.* 406 (2021), 126848.
- [127] S. Varjani, P. Rakholiya, H.Y. Ng, S. You, J.A. Teixeira, Microbial degradation of dyes: an overview, *Bioresour. Technol.* 314 (2020), 123728.
- [128] M. Parvaz, N. Salah, Z.H. Khan, Photocatalytic properties of TiS₂ nanodisc and Sb@TiS₂ nanocomposite for methylene blue dye, *Optik* 207 (2020), 163810.
- [129] Y. Liu, X. She, X. Zhang, C. Liang, J. Wu, P. Yu, Y. Nakanishi, B. Xie, H. Xu, Pulickel M. Ajayan, W. Yang, Metallic 1T-TiS₂ nanodots anchored on a 2D graphitic C₃N₄ nanosheet nanostructure with high electron transfer capability for enhanced photocatalytic performance, *RSC Adv.* 7 (2017), 55269.
- [130] H.Y. He, Solvothermal synthesis and photocatalytic activity of S-doped TiO₂ and TiS₂ powders, *Res. Chem. Intermed.* 36 (2010) 155.
- [131] P.J. Rosy, M.J.S. Jas, K. Santhanalakshmi, M. Murugan, P. Manivannan, Expert development of Hetero structured TiS₂-TiO₂ nanocomposites and evaluation of electron acceptors effect on the photo catalytic degradation of organic Pollutants under UV-light, *J. Mater. Sci. Mater. Electron.* 32 (2021) 4053.
- [132] M.-Y. Li, Y. Shi, C.-C. Cheng, L.-S. Lu, Y.-C. Lin, H.-L. Tang, M.-L. Tsai, C.-W. Chu, K.-H. Wei, J.-H. He, W.-H. Chang, K. Suenaga, L.-J. Li, Epitaxial growth of a monolayer WSe₂-MoS₂ lateral p-n junction with an atomically sharp interface, *Science* 349 (2015) 524.
- [133] Q. Ji, Y. Zhang, Y. Zhang, Z. Liu, Chemical vapour deposition of group-VIB metal dichalcogenide monolayers: engineered substrates from amorphous to single crystalline, *Chem. Soc. Rev.* 44 (2015) 2587.
- [134] A.C. Ferrari, F. Bonaccorso, V. Fal'ko, K.S. Novoselov, S. Roche, P. Bøggild, S. Borini, F.H.L. Koppens, V. Palermo, N. Pugno, J.A. Garrido, R. Sordan, A. Bianco, L. Ballerini, M. Prato, E. Lidorikis, J. Kivioja, C. Marinelli, T. Ryhänen, A. Morpurgo, J.N. Coleman, V. Nicolosi, L. Colombo, A. Fert, M. Garcia-Hernandez, A. Bachtold, G.F. Schneider, F. Guinea, C. Dekker, M. Barbone, Z. Sun, C. Galiotis, A.N. Grigorenko, G. Konstantatos, A. Kis, M. Katsnelson, L. Vandersypen, A. Loiseau, V. Morandi, D. Neumaier, E. Treossi, V. Pellegrini, M. Polini, A. Tredicucci, G.M. Williams, B. Hee Hong, J.-H. Ahn, J. Min Kim, H. Zirath, B.J. van Wees, H. van der Zant, L. Occhipinti, A. Di Matteo, I.A. Kinloch, T. Seyller, E. Quesnel, X. Feng, K. Teo, N. Rupasinghe, P. Hakonen, S.R.T. Neil, Q. Tannock, T. Löfwander, J. Kinnaret, Science and technology roadmap for graphene, related two-dimensional crystals, and hybrid systems, *Nanoscale* 7 (2015) 4598.
- [135] Y. Shi, H. Li, L.-J. Li, Recent advances in controlled synthesis of two-dimensional transition metal dichalcogenides via vapour deposition techniques, *Chem. Soc. Rev.* 44 (2015) 2744.
- [136] Y. Wang, A. Pham, S. Li, J. Yi, Electronic and magnetic properties of transition-metal-doped monolayer black phosphorus by defect engineering, *J. Phys. Chem. C* 120 (2016) 9773.
- [137] A.A. Tedstone, D.J. Lewis, P. O'Brien, Synthesis, properties, and applications of transition metal-doped layered transition metal dichalcogenides, *Chem. Mater.* 28 (2016) 1965.
- [138] M. Manickam, D.R.G. Mitchell, P. Singh, TEM investigation of MnO₂ cathode containing TiS₂ and its influence in aqueous lithium secondary battery, *Electrochim. Acta* 52 (2007) 3294.
- [139] C. Lee, Y.-T. Jeong, P.M. Nogaes, H.-Y. Song, Y. Kim, R.-Z. Yin, S.-K. Jeong, Electrochemical intercalation of Ca²⁺ ions into TiS₂ in organic electrolytes at room temperature, *Electrochem. Commun.* 98 (2019) 115.
- [140] R. Elazari, G. Salitra, G. Gershinsky, A. Garsuch, A. Panchenko, D. Aurbach, Li ion cells comprising lithiated columnar silicon film anodes, TiS₂ cathodes and fluoroethylene carbonate (FEC) as a critically important component, *J. Electrochem. Soc.* 159 (2012) A1440.
- [141] D.S. Tchitcheikova, A. Ponrouch, R. Verrilli, T. Broux, C. Frontera, A. Sorrentino, F. Bardé, N. Biskup, M.E. Arroyo-de Dompablo, M.R. Palacín, Electrochemical intercalation of calcium and magnesium in TiS₂: fundamental studies related to multivalent battery applications, *Chem. Mater.* 30 (2018) 847.
- [142] H.-S. Ryu, J.-S. Kim, J.-S. Park, J.-W. Park, K.-W. Kim, J.-H. Ahn, T.-H. Nam, G. Wang, H.-J. Ahn, Electrochemical properties and discharge mechanism of Na/TiS₂ cells with liquid electrolyte at room temperature, *J. Electrochem. Soc.* 160 (2013) A338.
- [143] Y. Zhou, J. Wan, Q. Li, L. Chen, J. Zhou, H. Wang, D. He, X. Li, Y. Yang, H. Huang, Chemical welding on semimetallic TiS₂ nanosheets for high-performance flexible n-type thermoelectric films, *ACS Appl. Mater. Interfaces* 9 (2017), 42430.
- [144] R. Li, J. Dui, Y. Fu, Y. Xu, S. Zhou, Ultrahigh power factor and enhanced thermoelectric performance of individual Te/TiS₂ nanocables, *Nanotechnology* 27 (2016), 415704.
- [145] C. Wan, R. Tian, A.B. Azizi, Y. Huang, Q. Wei, R. Sasai, S. Wasusate, T. Ishida, K. Koumoto, Flexible thermoelectric foil for wearable energy harvesting, *Nano Energy* 30 (2016) 840.
- [146] Y. Wang, J. Wen, Z. Fan, N. Bao, R. Huang, R. Tu, Y. Wang, Energy-filtering-induced high power factor in PbS-nanoparticles-embedded TiS₂, *AIP Adv.* 5 (2015), 047126.
- [147] E. Guilmeau, Y. Bréard, A. Maignan, Transport and thermoelectric properties in Copper intercalated TiS₂ chalcogenide, *Appl. Phys. Lett.* 99 (2011), 052107.
- [148] E. Guilmeau, T. Barbier, A. Maignan, D. Chateigner, Thermoelectric anisotropy and texture of intercalated TiS₂, *Appl. Phys. Lett.* 111 (2017), 133903.
- [149] C. Yin, Q. Hu, G. Wang, T. Huang, X. Zhou, X. Zhang, Y. Dou, B. Kang, J. Tang, N. Liu, R. Ang, Intriguing substitution of conducting layer triggered enhancement of thermoelectric performance in misfit-layered (SnS)_{1.2}(TiS₂)₂, *Appl. Phys. Lett.* 110 (2017), 043507.
- [150] Y.E. Putri, C. Wan, R. Zhang, T. Mori, K. Koumoto, Thermoelectric performance enhancement of (BiS)_{1.2}(TiS₂)₂ misfit layer sulfide by chromium doping, *J. Adv. Ceram.* 2 (2013) 42.
- [151] Y. Ye, Y. Wang, Y. Shen, Y. Wang, L. Pan, R. Tu, C. Lu, R. Huang, K. Koumoto, Enhanced thermoelectric performance of xMoS₂-TiS₂ nanocomposites, *J. Alloys Compd.* 666 (2016) 346.
- [152] J. Zhang, Y. Ye, C. Li, J. Yang, H. Zhao, X. Xu, R. Huang, L. Pan, C. Lu, Y. Wang, Thermoelectric properties of TiS₂-xPbSnS₃ nanocomposites, *J. Alloys Compd.* 696 (2017) 1342.
- [153] R. Daou, H. Takahashi, S. Hébert, M. Beaumale, E. Guilmeau, A. Maignan, Intrinsic effects of substitution and intercalation on thermal transport in two-dimensional TiS₂ single crystals, *J. Appl. Phys.* 117 (2015), 165101.
- [154] J. Zhang, X.Y. Qin, H.X. Xin, D. Li, C.J. Song, Thermoelectric properties of Co-doped TiS₂, *J. Electron. Mater.* 40 (2011) 980.
- [155] M. Beaumale, T. Barbier, Y. Bréard, B. Raveau, Y. Kinemuchi, R. Funahashi, E. Guilmeau, Mass fluctuation effect in Ti_{1-x}Nb_xS₂ bulk compounds, *J. Electron. Mater.* 43 (2014) 1590.
- [156] A. Ramakrishnan, S. Raman, L.-C. Chen, K.-H. Chen, Enhancement in thermoelectric properties of TiS₂ by Sn addition, *J. Electron. Mater.* 47 (2018) 3091.
- [157] T. Aoki, C. Wan, H. Ishiguro, H. Morimitsu, K. Koumoto, Evaluation of layered TiS₂-based thermoelectric elements fabricated by a centrifugal heating technique, *J. Ceram. Soc. Jpn.* 119 (2011) 382.
- [158] C. Bourges, T. Barbier, G. Guélou, P. Vaqueiro, A.V. Powell, O.I. Lebedev, N. Barrier, Y. Kinemuchi, E. Guilmeau, Thermoelectric properties of TiS₂ mechanically alloyed compounds, *J. Eur. Ceram. Soc.* 36 (2016) 1183.
- [159] C. Wan, Y. Wang, N. Wang, K. Koumoto, Low-thermal-conductivity (MS)_{1+x}(TiS₂)₂ (M = Pb, Bi, Sn) misfit layer compounds for bulk thermoelectric materials, *Materials* 3 (2010).
- [160] C. Wan, Y. Kodama, M. Kondo, R. Sasai, X. Qian, X. Gu, K. Koga, K. Yabuki, R. Yang, K. Koumoto, Dielectric mismatch mediates carrier mobility in organic-intercalated layered TiS₂, *Nano Lett.* 15 (2015) 6302.
- [161] S. Ferhat, C. Domain, J. Vidal, D. Noël, B. Ratier, B. Lucas, Flexible thermoelectric device based on TiS₂(HA)_x n-type nanocomposite printed on paper, *Org. Electron.* 68 (2019) 256.
- [162] F. Pawula, R. Daou, S. Hébert, O. Lebedev, A. Maignan, A. Subedi, Y. Kakefuda, N. Kawamoto, T. Baba, T. Mori, Anisotropic thermal transport in magnetic intercalates Fe_xTiS₂, *Phys. Rev. B* 99 (2019), 085422.
- [163] Y.E. Putri, C. Wan, Y. Wang, W. Norimitsu, M. Kusunoki, K. Koumoto, Effects of alkaline earth doping on the thermoelectric properties of misfit layer sulfides, *Scripta Mater.* 66 (2012) 895.
- [164] G. Li, K. Yao, G. Gao, Strain-induced enhancement of thermoelectric performance of TiS₂ monolayer based on first-principles phonon and electron band structures, *Nanotechnology* 29 (2017), 015204.
- [165] S. Jacob, B. Delatouche, D. Péré, Z. Ullah Khan, M.J. Ledoux, X. Crispin, R. Chmielowski, High-performance flexible thermoelectric modules based on high crystal quality printed TiS₂/hexylamine, *Sci. Technol. Adv. Mater.* 22 (2021) 907.
- [166] X. Li, X. Ding, Y. Li, L. Wang, J. Fan, A TiS₂ nanosheet enhanced fluorescence polarization biosensor for ultra-sensitive detection of biomolecules, *Nanoscale* 8 (2016) 9852.
- [167] N. Dhenadhayalan, M.I. Sriram, K.-C. Lin, Aptamer-based fluorogenic sensing of interferon-gamma probed with ReS₂ and TiS₂ nanosheets, *SENSOR ACTUAT B-CHEM* 258 (2018) 929.
- [168] X. Zhu, S. Chen, M. Zhang, L. Chen, Q. Wu, J. Zhao, Q. Jiang, Z. Zheng, H. Zhang, TiS₂-based saturable absorber for ultrafast fiber lasers, *Photon. Res.* 6 (2018) C44.
- [169] Q. Song, Z. Wu, P. Ma, GuojuWang, B. Zhang, TiS₂, MoS₂, WS₂/Sb₂Te₃ mixed nanosheets saturable absorber for dual-wavelength passively Q-switched Nd:GYSGG Laser, *Infrared Phys. Technol.* 92 (2018) 1.
- [170] X. Gan, H. Zhao, S. Chen, H. Yu, X. Quan, Three-dimensional porous HxTiS₂ nanosheet-polyaniline nanocomposite electrodes for directly detecting trace Cu(II) ions, *Anal. Chem.* 87 (2015) 5605.